

Chapter 8: Channel and Pipe Flow (Chap. 7 Bernard)

Channel, pipe, and BL flows similar due to wall boundaries, especially near wall, however some differences due to differences in their outer flows.

Pipe curvature effects are not discernable.

Channel flow experiments are difficult due requirement large span with 2D mean flow vs. DNS which can use periodic boundary conditions. Whereas pipe flow is amendable to both.

BL amendable both experiments and DNS and better for experimental study of coherent structures and transition to fully turbulent flow.

Pat 1: Channel flow

Flow between two parallel plates, with constant P_x : Poiseuille flow.

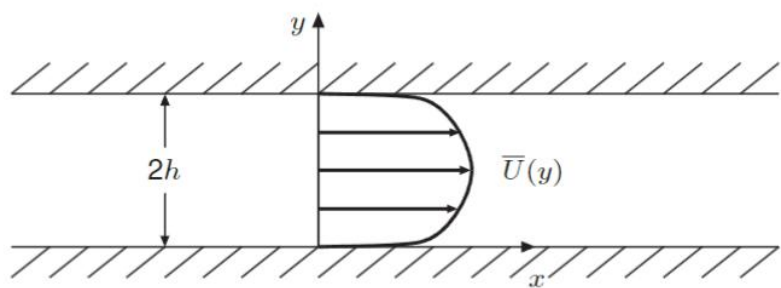


Figure 7.1 Geometry of channel flow.

For fully developed laminar flow:

$$U(y) = -\frac{1}{2\mu} \frac{\partial P}{\partial x} y(2h - y)$$

This solution holds for $Re = hU_m/\nu < 1000$, where:

$$U_m = \frac{1}{2h} \int_0^{2h} \bar{U}(y) dy = \text{mean bulk velocity}$$

For turbulent flow $\bar{\underline{U}} = (\bar{U}(y), 0, 0)$ and $\underline{u} = (u, v, w)$.

Periodic BCs in x, z assuming large enough domain such that, e.g., $f(r) \rightarrow 0$ for large r .

Channel flow simulations characterized using:

$$R_\tau = \frac{U_\tau h}{\nu} = \frac{h}{(\nu/U_\tau)}$$

h = length scale channel
 $\frac{\nu}{U_\tau}$ = viscous length scale = size flow features near wall viscous region

Based on the friction velocity

$$U_\tau = \sqrt{\frac{\tau_w}{\rho}}$$

Where:

$$\tau_w = \mu \frac{d\bar{U}}{dy}(0)$$

Is the wall shear stress.

For large R_τ clear separation inner and outer flow.

R_e	3300	125000
R_τ	180	5186
DNS (year)	1987	2015

Reynolds Stress and Force Balance

For fully developed mean flow, momentum equations become:

$$0 = -\frac{\partial \bar{P}}{\partial x} + \frac{d}{dy} \left(\mu \frac{d\bar{U}}{dy} - \rho \bar{uv} \right) = -\frac{\partial \bar{P}}{\partial x} + \frac{d\tau}{dy} \quad (1) \quad \boxed{x \text{ -direction}}$$

$$\tau = \mu \frac{d\bar{U}}{dy} - \rho \bar{uv} = \text{Total mean shear stress}$$

$$0 = -\frac{\partial \bar{P}}{\partial y} - \rho \frac{d\bar{v}^2}{dy} \quad (2) \quad \boxed{y \text{ -direction}}$$

$$0 = 0 \quad \boxed{z \text{ -direction}}$$

Note that $\bar{U}, \bar{u}^2, \bar{v}^2, \bar{w}^2, \bar{uv} = f(y)$.

Taking an x derivative of Eqs. (1) and (2) shows that

$$\frac{\partial \bar{P}}{\partial x} \neq f(x, y) = \text{constant (i.e., } \bar{P}_{xx} = \bar{P}_{yx} = \bar{P}_{xy} = 0)$$

Integration of Eq. (2) across the channel from 0 to y :

$$\bar{P}(x, y) = \bar{P}(x, 0) - \rho \bar{v}^2(y)$$

Since $\bar{v}^2(0) = 0$, showing that $\bar{P}(x, y)$ is minimum where $\bar{v}^2(y)$ is maximum, which differs from laminar flow where the pressure is constant across the flow.

Also, since $\frac{\partial \bar{P}}{\partial x} = \text{constant}$,

$$\bar{P}(x, y) - \bar{P}(x + L, y) \neq f(y)$$

Integration of Eq. (1) over the area $0 \leq x \leq L, 0 \leq y \leq 2h$ yields force balance:

$$\int_0^L \int_0^{2h} 0 \, dx dy = \int_0^L \int_0^{2h} \left[-\frac{\partial \bar{P}}{\partial x} + \frac{d}{dy} \left(\mu \frac{d\bar{U}}{dy} - \rho \overline{uv} \right) \right] dx dy$$

$$\Delta \bar{P} 2h - \tau_w 2L = 0 \quad (3a)$$

Where:

$$\Delta \bar{P} = -L \frac{\partial \bar{P}}{\partial x} = \bar{P}(x, 0) - \bar{P}(x + L, 0)$$

Is the pressure drop between x locations. Note that in deriving Eq. (3) the channel centerline asymmetry condition was used:

$$\frac{d\bar{U}}{dy}(0) = -\frac{d\bar{U}}{dy}(2h)$$

Eq. (3) shows that pressure force is balanced by τ_w force. For turbulent flow, channel center high momentum fluid is better able to penetrate wall region vs. laminar flow resulting in steeper velocity gradient near the wall.

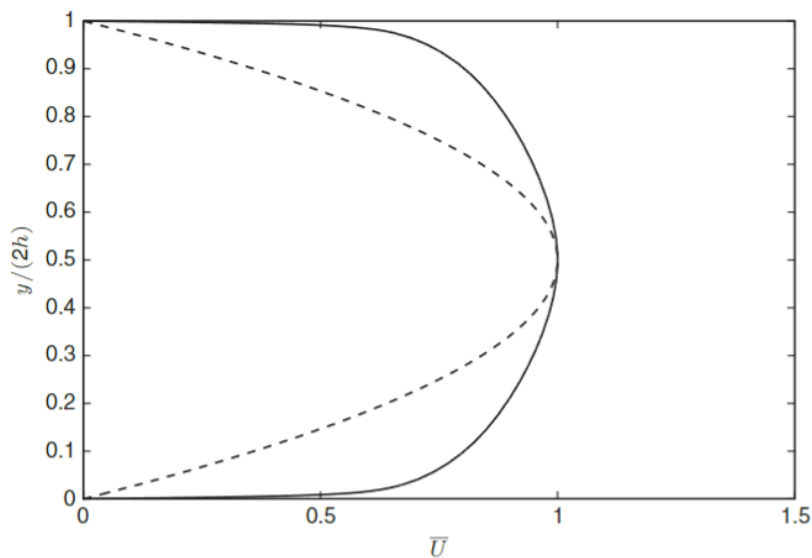


Figure 7.2 Average velocity in channel flow of width $2h$ scaled by mean centerline velocity, U_c : —, turbulent flow; ---, laminar flow.

Differentiating the velocity profile of fully developed laminar flow [$U(y) = -\frac{1}{2\mu} \frac{\partial P}{\partial x} y(2h - y)$] and substituting $\tau_w = \mu \frac{dU}{dy}(0)$ gives:

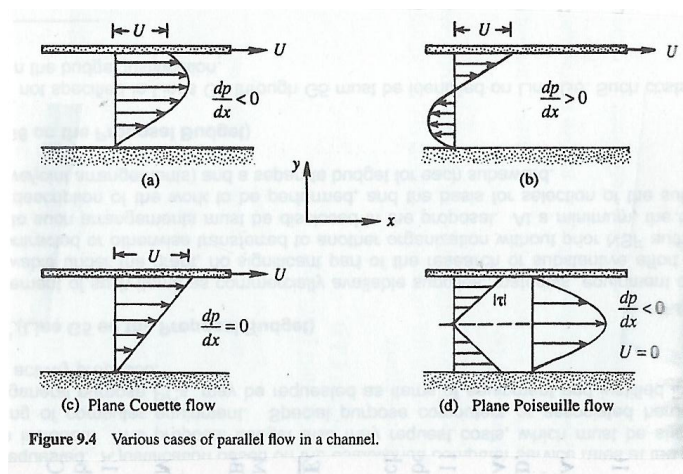
$$\begin{aligned} \frac{dU}{dy} &= -\frac{1}{2\mu} \frac{\partial P}{\partial x} (2h - 2y) = -\frac{1}{\mu} \frac{\partial P}{\partial x} (h - y) \\ &= -\frac{1}{\mu} \frac{\partial P}{\partial x} h \left(1 - \frac{y}{h}\right) \end{aligned}$$

$$\begin{aligned} \mu U_{yy} &= \tau_y = P_x \\ \tau &= \mu U_y \end{aligned}$$

$$\begin{aligned} \frac{dU}{dy}(0) &= -\frac{1}{\mu} \frac{\partial P}{\partial x} h = \frac{\tau_w}{\mu} \rightarrow -\frac{\partial P}{\partial x} = \frac{\tau_w}{h} \\ \tau_w &= -h \frac{\partial P}{\partial x} \end{aligned}$$

$$\mu \frac{dU}{dy} = -h \frac{\partial P}{\partial x} \left(1 - \frac{y}{h}\right) = \tau_w \left(1 - \frac{y}{h}\right)$$

i.e., the shear stress $\tau_{12} = \mu \frac{dU}{dy}$ is linear across the channel: momentum flux (shear stress) across channel from the centerline towards walls due to $-P_x$.



For turbulent flow:

$$-L \frac{\partial \bar{P}}{\partial x} 2h - 2\tau_w L = 0 \quad (3b)$$

$$-\frac{\partial \bar{P}}{\partial x} = \frac{\tau_w}{h} = \text{constant} \quad (4)$$

Substituting Eq. (4) into Eq. (1) and integrating from 0 to y , gives:

$$0 = \int_0^y \left[\frac{\tau_w}{h} + \frac{d}{dy} \left(\mu \frac{d\bar{U}}{dy} - \rho \bar{u}\bar{v} \right) \right] dy$$

$$0 = \frac{\tau_w}{h} y + \left[\mu \frac{d\bar{U}}{dy} - \rho \bar{u}\bar{v} \right]_0^y$$

$$0 = \frac{\tau_w}{h} y - \tau_w + \mu \frac{d\bar{U}}{dy} - \rho \bar{u}\bar{v}$$

$$\mu \frac{d\bar{U}}{dy} - \rho \bar{u}\bar{v} = \tau_w \left(1 - \frac{y}{h} \right) \quad (5)$$

i.e., same as laminar flow, with the addition of $-\rho \bar{u}\bar{v}$. i.e., the sum of viscous and turbulent stress varies linearly across the channel.

Eq. (5) can be scaled using the friction velocity, such that:

$$\nu \frac{d\bar{U}}{dy} - \overline{uv} = U_\tau^2 \left(1 - \frac{y}{h}\right)$$

$$\nu \frac{d\bar{U}^+}{dy} - \frac{\overline{uv}}{U_\tau} = U_\tau \left(1 - \frac{y}{h}\right)$$

$$\nu \frac{d\bar{U}^+}{dy^+} \frac{U_\tau}{\nu} - \frac{\overline{uv}}{U_\tau} = U_\tau \left(1 - \frac{y}{h}\right)$$

$$\frac{d\bar{U}^+}{dy^+} - \overline{uv}^+ = 1 - \frac{y}{h} = 1 - \frac{y^+ \nu U_\tau}{U_\tau \nu R_\tau}$$

$$R_\tau = \frac{U_\tau h}{\nu}$$

$$\frac{d\bar{U}^+}{dy^+} - \overline{uv}^+ = 1 - \frac{y^+}{R_\tau} = \bar{\tau}^+ = \text{total scaled mean shear stress (of course also linear)}$$

Where:

$$\bar{U}^+ = \frac{\bar{U}}{U_\tau} \quad \overline{uv}^+ = \frac{\overline{uv}}{U_\tau^2} \quad y^+ = \frac{U_\tau y}{\nu}$$

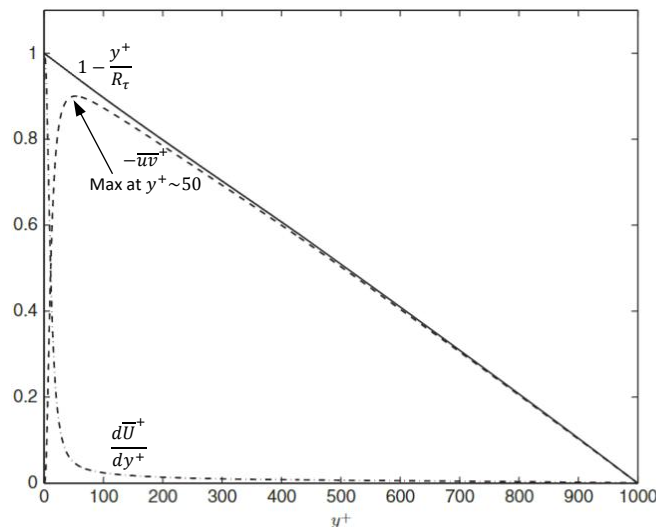


Figure 7.3 Decomposition of the total stress as given by Eq. (7.14) in turbulent channel flow: \cdots , $d\bar{U}^+/dy^+$; $---$, $-\overline{uv}^+$; $-$, $1 - y^+/R_\tau$. Data taken from [13].

The mean viscous (molecular) momentum transport/flux is confined to a thin layer near the wall. The drop in molecular momentum transport/flux is compensated by the turbulent momentum transport/flux, which is asymmetric across the channel. The peak in $-\overline{uv}^+$ is at $y^+ \approx 53$ after which it has a nearly linear variation to zero at the channel centerline where the mean shear is zero.

Eq. (1) scaling:

$$0 = \frac{\tau_w}{h} + \frac{d}{dy} \left(\mu \frac{d\bar{U}}{dy} - \rho \overline{uv} \right)$$

$$0 = \frac{\rho U_\tau^2}{h} + \frac{d}{dy} \left(\mu \frac{d\bar{U}}{dy} - \rho \overline{uv} \right)$$

$$0 = \frac{U_\tau^2}{h} + \frac{d}{dy^+} \frac{U_\tau}{\nu} \left(\nu \frac{d\bar{U}}{dy^+} \frac{U_\tau}{\nu} - \overline{uv} \right)$$

$$0 = \frac{\nu U_\tau}{h} + \frac{d}{dy^+} \left(U_\tau \frac{d\bar{U}}{dy^+} - \overline{uv} \right)$$

$$0 = \frac{\nu U_\tau}{h} + U_\tau \frac{d}{dy^+} \left(\frac{d\bar{U}}{dy^+} - \frac{\overline{uv}}{U_\tau} \right)$$

$$0 = \frac{\nu}{h U_\tau} + \frac{d}{dy^+} \left(\frac{1}{U_\tau} \frac{d\bar{U}}{dy^+} - \frac{\overline{uv}}{U_\tau^2} \right)$$

$$0 = \frac{1}{R_\tau} + \frac{d}{dy^+} \left(\frac{d\bar{U}^+}{dy^+} - \overline{uv}^+ \right)$$

$$U_\tau = \sqrt{\frac{\tau_w}{\rho}}$$

$$y^+ = \frac{U_\tau y}{\nu}$$

$$\frac{d}{dy} = \frac{d}{dy^+} \frac{U_\tau}{\nu}$$

$$R_\tau = \frac{U_\tau h}{\nu}$$

$$\bar{U}^+ = \frac{\bar{U}}{U_\tau}$$

0 = (1) pressure force + (2) viscous force – (3) turbulence force

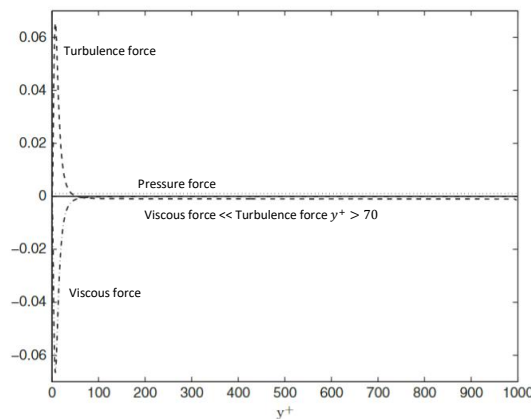


Figure 7.4 Decomposition of the mean momentum equation (7.16) in turbulent channel flow: - · - ·, viscous force; - - -, turbulent transport; · · · ·, pressure force. Data taken from [13].

Pressure force (1) Is constant across channel and balanced by (3) for $y^+ \geq$ approximately 70.

Near wall $y^+ \leq$ approximately 70, complex physics wherein (3) transports momentum from outer channel towards wall (gain), which is counterbalanced by viscous diffusion (2) again towards the wall (loss).

Mean Flow Similarity: Flow field regions.

- 1) Viscous sublayer: $f(\mu)$
- 2) Channel center = outer/core region $\neq f(\mu)$
- 3) Overlap layer = intermediate region, requires high Re for separation of 1) and 2).

Between 1) and 3) = buffer layer where turbulence is maximum: $5 \leq y^+ \leq 30$, as per later discussion.

Viscous sublayer (see Appendix A.1 for Taylor Series for u_i and $\langle u_i u_j \rangle$ near $y = 0$)

Viscosity is essential for flow near solid boundaries. Evaluating Eq. (1) at $y = 0$ and using Eq. (4) gives:

$$0 = \frac{\tau_w}{h} + \mu \frac{d^2 \bar{U}}{dy^2}(0) - \rho \frac{d\overline{uv}}{dy}(0) = \frac{\mu}{h} \frac{d\bar{U}}{dy}(0) + \mu \frac{d^2 \bar{U}}{dy^2}(0)$$

$$\frac{d^2 \bar{U}}{dy^2}(0) = -\frac{1}{h} \frac{d\bar{U}}{dy}(0) \quad (6)$$

Where the fact that

$$\frac{d\overline{uv}}{dy}(0) = 0$$

Follows from the identity:

$$\frac{\partial \overline{uv}}{\partial y} = \overline{\frac{\partial u}{\partial y} v} + u \overline{\frac{\partial v}{\partial y}}$$

Differentiating Eq. (1) with respect to y :

$$0 = -\frac{\partial \bar{P}}{\partial x} + \frac{d}{dy} \left(\mu \frac{d\bar{U}}{dy} - \rho \overline{uv} \right) \quad (1)$$

$$\frac{d^3 \bar{U}}{dy^3}(0) = 0 \quad (7)$$

Since

$$\begin{aligned}\frac{\partial^2 \overline{uv}}{\partial y^2}(0) &= 0 \\ \frac{\partial^2 \overline{uv}}{\partial y^2} &= \frac{\partial}{\partial y} \left(\overline{\frac{\partial u}{\partial y} v} + u \overline{\frac{\partial v}{\partial y}} \right) = 2 \overline{\frac{\partial u}{\partial y} \frac{\partial v}{\partial y}} + u \overline{\frac{\partial^2 v}{\partial y^2}} + \overline{\frac{\partial^2 u}{\partial y^2}} v \\ &= -2 \overline{\frac{\partial u}{\partial y} \frac{\partial u}{\partial x}} + u \overline{\frac{\partial^2 v}{\partial y^2}} + \overline{\frac{\partial^2 u}{\partial y^2}} v = 0 \text{ at } y = 0\end{aligned}$$

Using continuity $v_y = -u_x$ and $w_z = 0$.

Taylor series expansion for $\overline{U}(y)$ near $y = 0$:

$$\overline{U}(y) = \sum_{n=0}^{\infty} \frac{y^n}{n!} \frac{d^n \overline{U}}{dy^n}(0) \quad (8)$$

Substituting Eqs. (6) and (7) into (8) gives

$$\begin{aligned}\overline{U}(y) &= h \frac{d\overline{U}}{dy}(0) \frac{y}{h} + h^2 \frac{d^2 \overline{U}}{dy^2}(0) \frac{y^2}{2h^2} + o\left(\frac{y}{h}\right)^4 \\ \overline{U}(y) &\approx h \frac{d\overline{U}}{dy}(0) \frac{y}{h} - h \frac{d\overline{U}}{dy}(0) \frac{y^2}{2h^2} \\ \overline{U}(y) &\approx h \frac{d\overline{U}}{dy}(0) \left(\frac{y}{h} - \frac{y^2}{2h^2} \right) \quad (9)\end{aligned}$$

Scaling Eq. (9) with U_τ , yields

$$\overline{U}^+(y^+) = y^+ - \frac{(y^+)^2}{2R_\tau} + \dots$$

Which shows $\overline{U} = f(y, \tau_w, \rho, \nu)$; from dimensional analysis $\overline{U}^+ = \frac{\overline{U}}{U_\tau} = f(y^+)$; for small y^+ using Taylor Series $\overline{U}^+(y^+) = y^+ \neq f(R_e)$, i.e., complete similarity; and lastly from EFD and DNS valid for $y^+ < 5$.

Intermediate layer

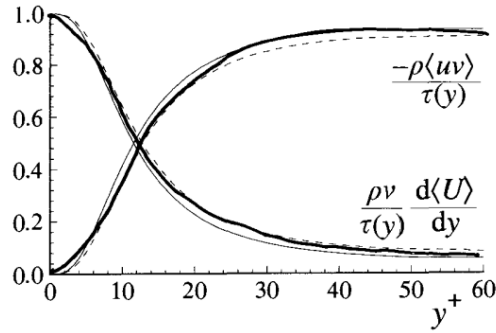


Fig. 7.4. Profiles of the fractional contributions of the viscous and Reynolds stresses to the total stress. DNS data of Kim *et al.* (1987): dashed lines, $Re = 5,600$; solid lines, $Re = 13,750$.

For $y^+ \geq 50 \rightarrow \frac{d\bar{U}^+}{dy^+} \ll \bar{uv}^+$ such that:

$$\frac{d\bar{U}^+}{dy^+} - \bar{uv}^+ = 1 - \frac{y^+}{R_\tau}$$

$$\bar{uv}^+ \approx -1$$

$$|\bar{uv}| \approx \frac{\tau_w}{\rho} \quad (9)$$

For large R_τ

Therefore, $\bar{U} \neq f(y)$, i.e., $\bar{U} = f(y, \tau_w, \rho, \dots)$ or similarly $\frac{d\bar{U}}{dy} = f(y, \tau_w, \rho, \dots)$ such that:

$$\frac{y}{U_\tau} \frac{d\bar{U}}{dy} = \text{constant}. \quad (10)$$

And assuming in the intermediate layer $y \frac{d\bar{U}}{dy} \approx \text{constant}$. Introducing a dimensionless constant of proportionality $k = 0.41$, known as the Von Karman constant, Eq. (10) becomes

$$\frac{d\bar{U}}{dy} = \frac{U_\tau}{ky} \quad (11)$$

Expressing Eq. (11) in wall units and integrating gives

$$\frac{1}{U_\tau} \frac{d\bar{U}}{dy} = \frac{1}{ky}$$

$$\frac{d\bar{U}^+}{dy^+} \frac{U_\tau}{\nu} = \frac{U_\tau}{ky^+\nu}$$

$$\frac{d\bar{U}^+}{dy^+} = \frac{1}{ky^+} \text{ (fundamental property (1) log-law region)}$$

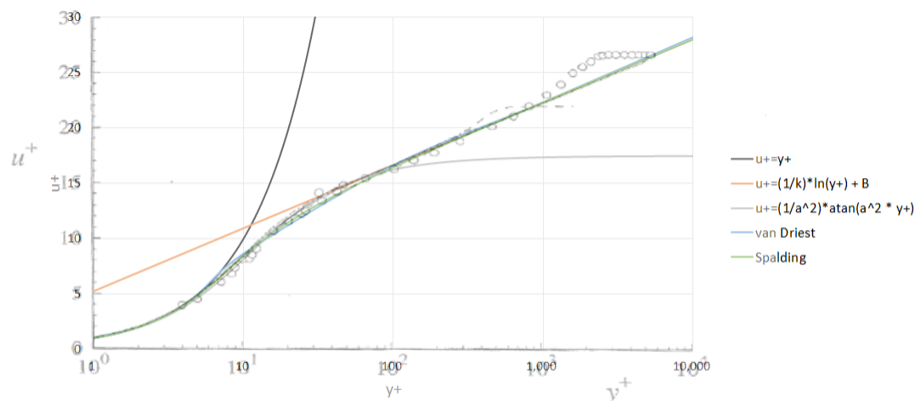
$$\int \frac{d\bar{U}^+}{dy^+} dy^+ = \int \frac{1}{ky^+} dy^+$$

$$\bar{U}^+(y^+) = \frac{1}{k} \log y^+ + B \quad (12)$$

$$k = 0.41$$

$$B = 5.2$$

Where $B \approx 5.2$ is a constant, which is determined by experiments.



Mean velocity profiles in wall units. Circles, boundary-layer experiments of Klebanoff (1954), $Re_\theta = 8,000$; dashed line, boundary-layer DNS of Spalart (1988), $Re_\theta = 1,410$; dot-dashed line, channel flow DNS of Kim *et al.* (1987), $Re = 13,750$; solid line, van Driest's law of the wall, Eqs. (7.144)–(7.145).

More precise determination of whether a log law is present can be obtained by examination of

$$\beta = y^+ \frac{d\bar{U}^+}{dy^+} = \frac{1}{k}$$

Which will be constant, and equal to $1/k$, in log-law regions if they exist.

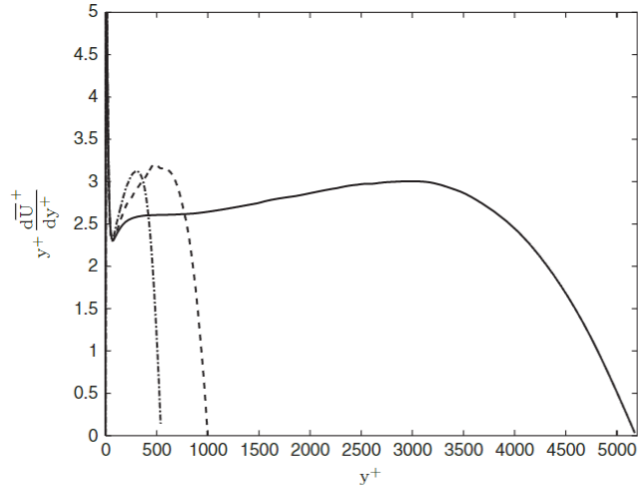


Figure 7.6 β as defined in Eq. (7.32) for the mean velocities in Figure 7.5. \cdots , $R_\tau = 541$; $---$, $R_\tau = 1000$; $-$, $R_\tau = 5186$. Data from [10, 13].

β constant only for $R_\tau = 5186 \rightarrow$ intermediate layer developed only for $R_\tau > 2200$.

Buffer layer: Merges smoothly with the viscosity-dominated sub-layer and turbulence-dominated log-layer in the region $5 < y^+ \leq 30$. Unified Inner layer: There are several ways to obtain composite of sub-/buffer and log-layers.

Evaluating $\langle uv \rangle$ near the wall (Appendix A.1) shows that:

$$\langle uv \rangle \sim y^3 \quad y \rightarrow 0$$

Several expressions which satisfy this requirement have been derived and are commonly used in turbulent-flow analysis, e.g., Spalding (Appendix A.2) using the following assumptions:

1. Passes through $y^+ = 0$ at $\bar{U}^+ = 0$.
2. Is tangent at this point to $y^+ = \bar{U}^+$
3. Is asymptotic at large y^+ to $\bar{U}^+(y^+) = 2.5 \log y^+ + 5.5$
4. Fits the experimental points at intermediate y^+ values

$$\bar{U}^+ = y^+ - e^{-\kappa B} \left[e^{\kappa \bar{U}^+} - 1 - \kappa \bar{U}^+ - \frac{(\kappa \bar{U}^+)^2}{2} - \frac{(\kappa \bar{U}^+)^3}{6} \right]$$

Fig. 6-11 shows a comparison of this equation with experimental data obtained very close to the wall. The agreement is excellent. It should be recognized that obtaining data this close to the wall is very difficult.

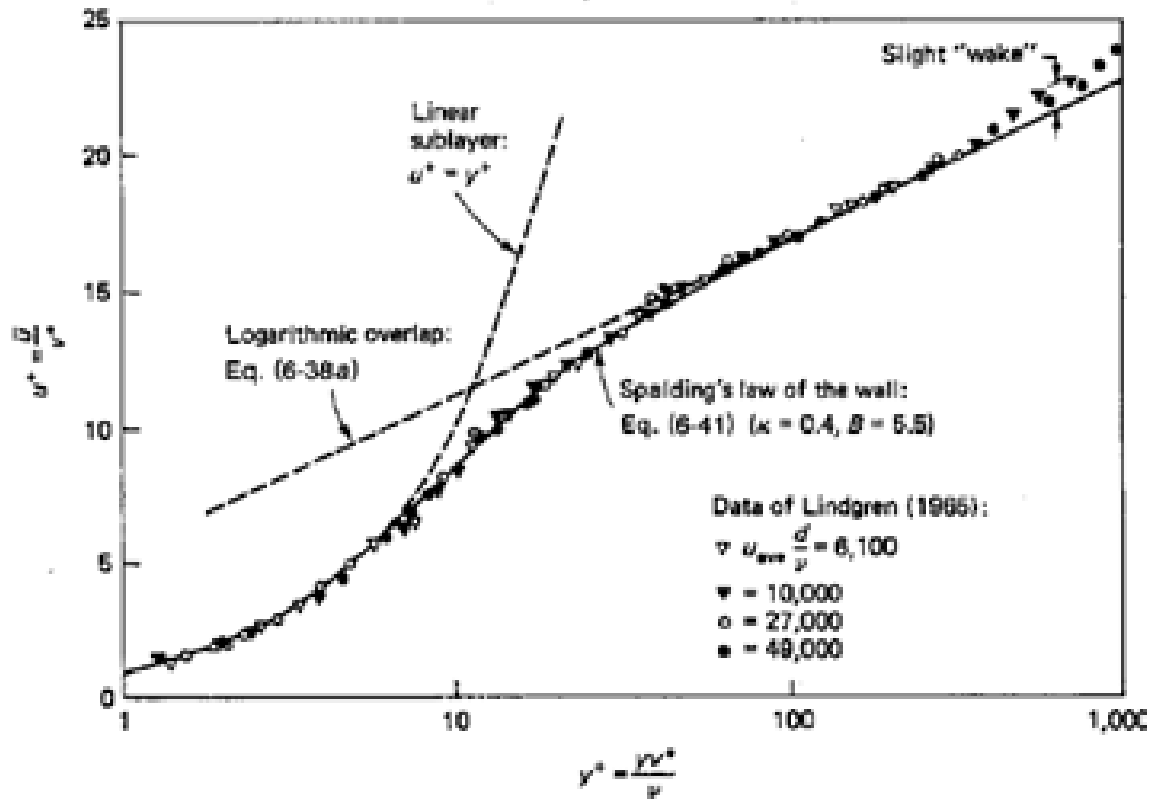


FIGURE 6-11
Comparison of Spalding's inner-law expression with the pipe-flow data of Lindgren (1965).

Velocity moments

Effect of Re negligible in core region of the channel.

Near wall, for larger R_τ , more rapid changes in correlations and shifted closer to the wall.

$\overline{v^2}$ damped near wall.

$\overline{v^2}$ and $\overline{w^2}$ somewhat isotropic in core region, but not $\overline{u^2}$.

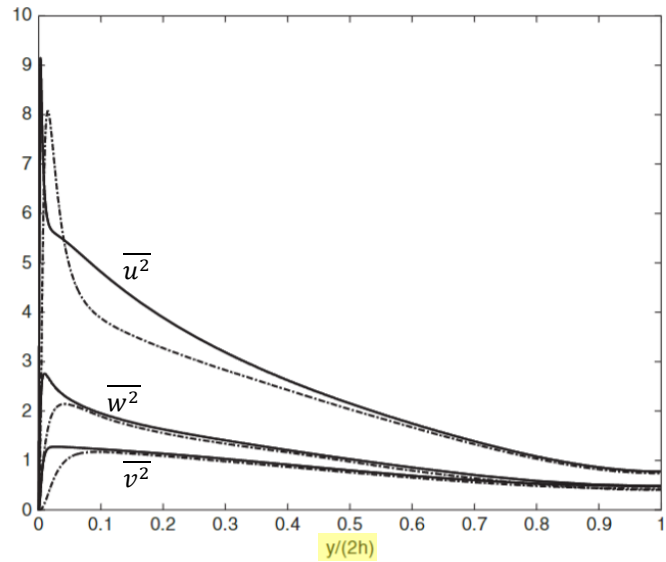


Figure 7.7 Normal Reynolds stresses in channel flow. —, $R_\tau = 5186$; - - -, $R_\tau = 1000$. Top curves are $\overline{u^2}$, middle curves are $\overline{w^2}$, lower curves are $\overline{v^2}$. Data taken from [10, 13].

$\overline{u^2}_{max} @ y^+ \sim 15.5$

Buffer layer: steep \overline{U}_y and max $\overline{u_i u_j}$

For $y^+ < 2.5$ results seem independent of R_e . However, for $R_\tau = 5186$:

$$\frac{du_{rms}^+}{dy^+}(0) = 0.5$$

$$\frac{d^2 u_{rms}^+}{dy^{+2}}(0) = -0.038$$

$R_\tau = 1000$:

$$\frac{du_{rms}^+}{dy^+}(0) = 0.47$$

$$\frac{d^2 u_{rms}^+}{dy^{+2}}(0) = -0.032$$

i.e., persistent Reynolds number effect.

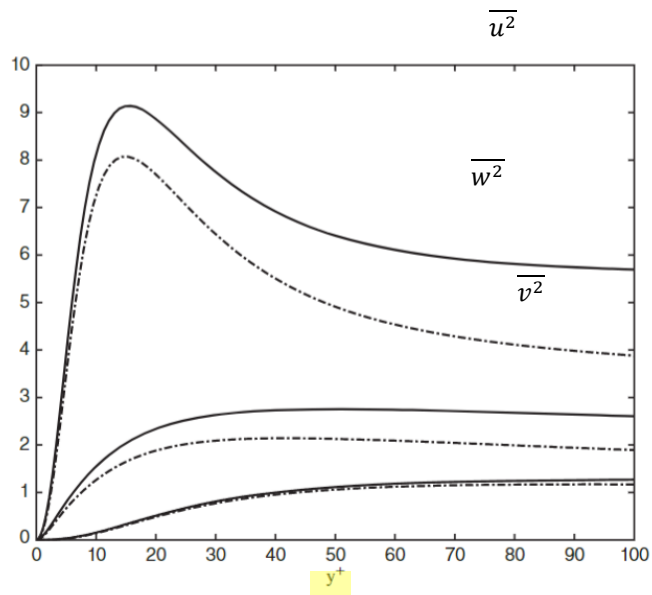


Figure 7.8 Normal Reynolds stresses in channel flow plotted with respect to y^+ . —, $R_\tau = 5186$; - - -, $R_\tau = 1000$. Top curves are $\overline{u^2}$, middle curves are $\overline{w^2}$, lower curves are $\overline{v^2}$. Data taken from [10, 13].

\bar{U}^+ is linear up to $y^+ = 5$, so consider a Taylor series expansion of $u_{rms}^+ = \sqrt{u^2}$ near $y = 0$:

$$u_{rms}^+ = \underbrace{u_{rms}^+(0)}_{\text{no-slip}} + \frac{du_{rms}^+}{dy^+}(0)y^+ + \frac{1}{2} \frac{d^2 u_{rms}^+}{dy^{+2}}(0)y^{+2} + O((y^+)^3) \quad (13)$$

The distance from the boundary over which u_{rms}^+ can be modeled as linear can be analyzed considering the ratio u_{rms}^+/\bar{U}^+ .

Recall scaling of $\bar{U}^+(y^+)$ resulted in the equation:

$$\begin{aligned} \bar{U}^+(y^+) &= \frac{\bar{U}(y)}{U_\tau} = y^+ - \frac{(y^+)^2}{2R_\tau} + O((y^+)^4) \\ \bar{U}^+(y^+) &\approx y^+ \left(1 - \frac{y^+}{2R_\tau}\right) \quad (14) \end{aligned}$$

Dividing Eq. (13) by \bar{U}^+ and combining with Eq. (14) gives:

$$\begin{aligned} \frac{u_{rms}^+}{\bar{U}^+} &= \frac{du_{rms}^+}{dy^+}(0) \frac{y^+}{\bar{U}^+} + \frac{1}{2} \frac{d^2 u_{rms}^+}{dy^{+2}}(0) \frac{y^{+2}}{\bar{U}^+} + O\left(\frac{(y^+)^3}{\bar{U}^+}\right) \\ \frac{u_{rms}^+}{\bar{U}^+} &= \frac{du_{rms}^+}{dy^+}(0) \frac{y^+}{y^+ \left(1 - \frac{y^+}{2R_\tau}\right)} + \frac{1}{2} \frac{d^2 u_{rms}^+}{dy^{+2}}(0) \frac{y^{+2}}{y^+ \left(1 - \frac{y^+}{2R_\tau}\right)} + O((y^+)^2) \end{aligned}$$

Define $y^{+'} = y^+/2R_\tau$

$$\frac{u_{rms}^+}{\bar{U}^+} = \frac{du_{rms}^+}{dy^+}(0) \frac{y^+}{y^+(1 - y^{+'})} + \frac{1}{2} \frac{d^2 u_{rms}^+}{dy^{+2}}(0) \frac{y^{+2}}{y^+(1 - y^{+'})} + O((y^+)^2)$$

and use binomial theorem such that:

$$\frac{1}{(1 - y^{+'})} \approx 1 + y^{+'}$$

Therefore,

$$\frac{u_{rms}^+}{\bar{U}^+} = \frac{du_{rms}^+}{dy^+}(0) \left(1 + \frac{y^+}{2R_\tau}\right) + \frac{1}{2} \frac{d^2u_{rms}^+}{dy^{+2}}(0) y^+ \left(1 + \frac{y^+}{2R_\tau}\right) + O((y^+)^2)$$

$$\frac{u_{rms}^+}{\bar{U}^+} = \frac{du_{rms}^+}{dy^+}(0) + y^+ \left(\frac{1}{2R_\tau} \frac{du_{rms}^+}{dy^+}(0) + \frac{1}{2} \frac{d^2u_{rms}^+}{dy^{+2}}(0) \right) + O((y^+)^2)$$

It follows that near the wall (see derivative relations pg. 15):

$$\frac{u_{rms}^+}{\bar{U}^+} = 0.5 + y^+ \left(\frac{0.25}{R_\tau} - 0.019 \right) + \dots \quad (*)$$

i.e., linearity maintained until $y^+ \approx 2$.

Similarly, spanwise rms fluctuations are given in the form:

$$w_{rms}^+ = \underbrace{w_{rms}^+(0)}_{\text{no-slip}} + \frac{dw_{rms}^+}{dy^+}(0) y^+ + \frac{1}{2} \frac{d^2w_{rms}^+}{dy^{+2}}(0) y^{+2} + O((y^+)^3)$$

And computations show that at the wall the approximate expression is:

$$w_{rms}^+ = 0.25y^+ + \dots \quad (**)$$

Using continuity, it can be shown that:

$$\frac{dv_{rms}^+}{dy^+} = 0$$

Such that, near the wall

$$v_{rms}^+ = \frac{1}{2} \frac{d^2v_{rms}^+}{dy^{+2}}(0) y^{+2} + O((y^+)^3)$$

Computations show that near the wall the approximate expression is:

$$v_{rms}^+ = 0.006y^{+2} + O((y^+)^3) \quad (***)$$

(*), (**), and (***) useful near-wall anisotropic turbulence modeling.

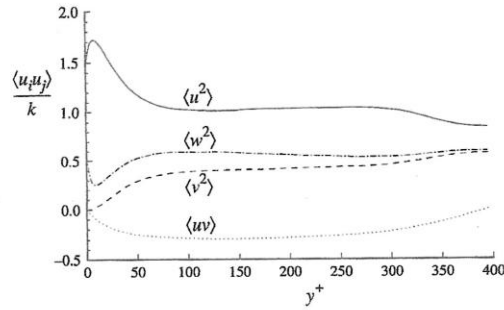


Fig. 7.15. Profiles of Reynolds stresses normalized by the turbulent kinetic energy from DNS of channel flow at $Re = 13,750$ (Kim *et al.* 1987).

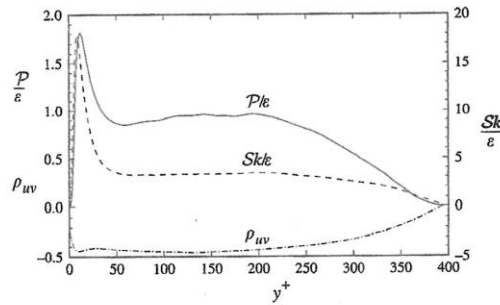


Fig. 7.16. Profiles of the ratio of production to dissipation (P/ϵ), normalized mean shear rate (Sk/ϵ), and shear stress correlation coefficient (ρ_{uv}) from DNS of channel flow at $Re = 13,750$ (Kim *et al.* 1987).

Table 7.2. Statistics in turbulent channel flow, obtained from the DNS data of Kim *et al.* (1987), $Re = 13,750$

	Location		
	Peak production $y^+ = 11.8$	Log law $y^+ = 98$	Centerline $y^+ = 395$
$\langle u^2 \rangle/k$	1.70	1.02	0.84
$\langle v^2 \rangle/k$	0.04	0.39	0.57
$\langle w^2 \rangle/k$	0.26	0.59	0.59
$\langle uv \rangle/k$	-0.116	-0.285	0
ρ_{uv}	-0.44	-0.45	0
Sk/ϵ	15.6	3.2	0
P/ϵ	1.81	0.91	0

Fundamental property (2) log-law region: $P/\epsilon \approx 1$

(3)

$$= \frac{-\langle uv \rangle}{k} \approx 0.3$$

TKE budget

Simplification of TKE equation obtained in Chapter 3 for channel flow yields:

$$0 = \underbrace{-\overline{uv} \frac{d\overline{U}}{dy}}_{\boxed{1}} - \underbrace{\varepsilon}_{\boxed{2}} - \underbrace{\frac{1}{\rho} \overline{pv}_y}_{\boxed{3}} + \underbrace{v \frac{d^2 k}{dy^2}}_{\boxed{4}} - \underbrace{\frac{1}{2} \frac{d\overline{vu_j^2}}{dy}}_{\boxed{5}}$$

- 1) Production
- 2) Dissipation
- 3) Pressure work/transport
- 4) Viscous diffusion/transport
- 5) Turbulent transport = $\frac{1}{2} \langle v \underline{u} \cdot \underline{u} \rangle_y$

For $y^+ > 30$ up to $y/2h = 1$, $P \approx \varepsilon$. (2)

P_{max} @ $y^+ = 12$ (near k peak), $P/\varepsilon \sim 1.8$

ε_{max} @ $y^+ = 0$, i.e., at the wall and has local plateau near P_{max} .

Turbulent transport (5) is important near the wall: negative for $8 < y^+ < 30$ and positive for $y^+ < 8$, which suggests much of the peak of the RS near $y^+ = 10$ is transported towards the wall.

At wall:

$$\varepsilon = v \frac{d^2 k}{dy^2}$$

i.e., dissipation equals molecular diffusion.

Most complex physics is in buffer layer $5 < y^+ < 30$.

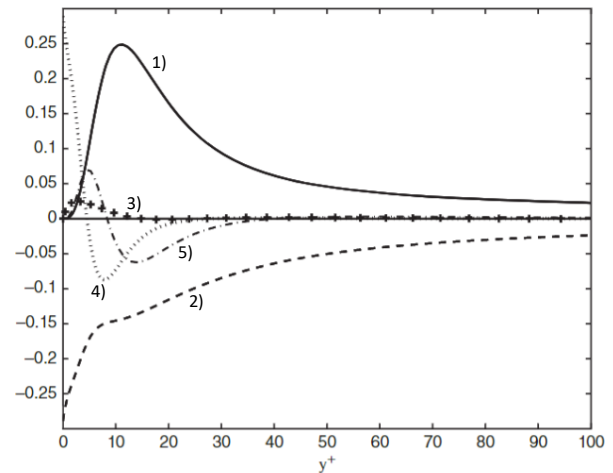


Figure 7.9 Turbulent kinetic energy budget in channel flow $R_\tau = 5186$ [10] scaled with v and u_τ ; —, production; ---, dissipation; +, pressure work; ···, viscous diffusion; - · - ·, turbulent transport.

Location of P_{max} can be estimated by rewriting the production term as:

$$-\overline{uv}^+ \frac{d\overline{U}^+}{dy^+} = \left(1 - \frac{y^+}{R_\tau} - \frac{d\overline{U}^+}{dy^+}\right) \frac{d\overline{U}^+}{dy^+} \quad (15)$$

P_{max} is located where d/dy^+ of Eq. (15) equals zero:

$$\begin{aligned} \frac{d}{dy^+} \left[\left(1 - \frac{y^+}{R_\tau} - \frac{d\overline{U}^+}{dy^+}\right) \frac{d\overline{U}^+}{dy^+} \right] &= 0 \\ \left(-\frac{1}{R_\tau} - \frac{d^2\overline{U}^+}{dy^{+2}} \right) \frac{d\overline{U}^+}{dy^+} + \left(1 - \frac{y^+}{R_\tau} - \frac{d\overline{U}^+}{dy^+}\right) \frac{d^2\overline{U}^+}{dy^{+2}} &= 0 \\ -\frac{1}{R_\tau} \frac{d\overline{U}^+}{dy^+} + \left(1 - \frac{y^+}{R_\tau} - 2 \frac{d\overline{U}^+}{dy^+}\right) \frac{d^2\overline{U}^+}{dy^{+2}} &= 0 \\ \left(1 - 2 \frac{d\overline{U}^+}{dy^+}\right) \frac{d^2\overline{U}^+}{dy^{+2}} &= 0 \end{aligned}$$

Where terms $O(R_\tau^{-1})$ are dropped.

Since $\frac{d^2\overline{U}^+}{dy^{+2}} \neq 0$ in the region of P_{max} , then

$$\frac{d\overline{U}^+}{dy^+} = \frac{1}{2} = -\overline{uv}^+ \quad (16)$$

$$\begin{aligned} \frac{d\overline{U}^+}{dy^+} - \overline{uv}^+ &= 1 - \frac{y^+}{R_\tau} \\ \text{If } y^+ \ll R_\tau &\rightarrow \\ \frac{d\overline{U}^+}{dy^+} - \overline{uv}^+ &= 1 \end{aligned}$$

Point where Eq. (16) is satisfied is visible in Fig. 7.3 at $y^+ \approx 12$.

ε budget

$$\frac{D\varepsilon}{Dt} = P_\varepsilon^1 + P_\varepsilon^2 + P_\varepsilon^3 + P_\varepsilon^4 + \Pi_\varepsilon + T_\varepsilon + D_\varepsilon - \Upsilon_\varepsilon$$

P_ε = production

Υ_ε = dissipation of dissipation

$\Pi_\varepsilon + T_\varepsilon + D_\varepsilon$ = redistribution

Like homogeneous shear flow for large y^+ (away from wall)

$$P_\varepsilon^4 \sim -\Upsilon_\varepsilon$$

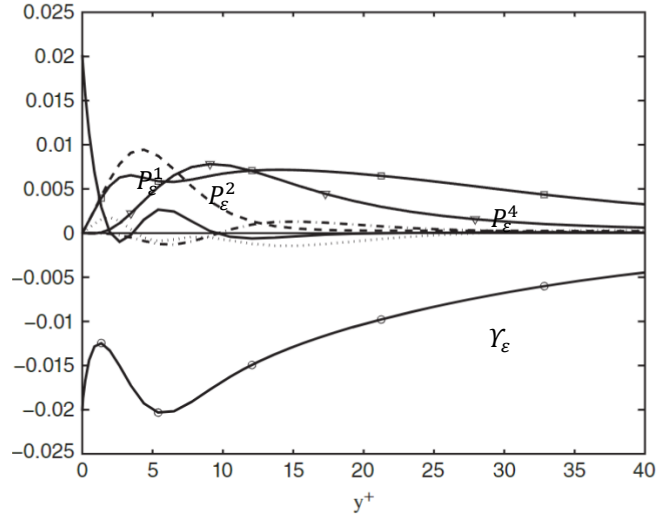


Figure 7.10 ε equation budget in channel flow at $R_\tau = 590$ [20] scaled with ν and u_τ . —, P_ε^1 ; - - -, P_ε^2 ; · · · ·, P_ε^3 ; □, P_ε^4 ; ○, $-\Upsilon_\varepsilon$; —, D_ε ; · · · ·, $\Pi_\varepsilon + T_\varepsilon$.

For $y^+ \leq 25$, P_ε^1 and P_ε^2 larger compared to P_ε^3 and $\Pi_\varepsilon + T_\varepsilon$.

Near wall $-\Upsilon_\varepsilon$ has minimum and at the wall $-\Upsilon_\varepsilon = D_\varepsilon$.

Evident ε behavior near the wall complex and challenge for modeling.

Reynolds Stress Budget (derived from RS transport equation)

$$\overline{u^2}: 0 = -2\overline{uv} \frac{d\overline{U}}{dy} - \varepsilon_{11} - \frac{d\overline{u^2v}}{dy} + \Pi_{11} + \nu \frac{d^2\overline{u^2}}{dy^2}$$

$$\overline{v^2}: 0 = -\varepsilon_{22} - \frac{d\overline{v^3}}{dy} + \Pi_{22} + \nu \frac{d^2\overline{v^2}}{dy^2} - \frac{2}{\rho} \frac{d\overline{pv}}{dy}$$

$$\overline{w^2}: 0 = -\varepsilon_{33} - \frac{d\overline{w^2v}}{dy} + \Pi_{33} + \nu \frac{d^2\overline{w^2}}{dy^2}$$

Where:

$$\varepsilon_{ij} = 2\nu \overline{\frac{\partial u_i}{\partial x_k} \frac{\partial u_j}{\partial x_k}} \quad \Pi_{ij} = \frac{1}{\rho} \overline{p \left(\frac{\partial u_i}{\partial x_j} + \frac{\partial u_j}{\partial x_i} \right)} = \frac{1}{\rho} \overline{p 2\Sigma_{ij}}$$

$$\Sigma_{ij} = \text{turbulent rate of strain} = \frac{1}{2}(u_{i,j} + u_{j,i})$$

Π_{ij} = pressure strain correlation

$\overline{u^2}$ connected mean flow via production term.

$\overline{v^2}$ and $\overline{w^2}$ production via Π_{22} and Π_{33} .

$\sum \Pi_{ii} = 0$, thus Π_{11} mostly < 0 .

Consequently, P in $\overline{u^2}$ is transferred to $\overline{v^2}$ and $\overline{w^2}$ via Π_{ii} .

Near wall $\Pi_{33} \sim \Pi_{11} + \Pi_{22}$

Near channel center:

$\overline{u^2}$: $P \sim \varepsilon_{11} + \Pi_{11}$

$\overline{v^2}$ and $\overline{w^2}$: $\varepsilon \sim \Pi_{22}$ and Π_{33} , respectively

Complex physics $y^+ < 40$

$\overline{u^2}$: $\varepsilon \sim \nu \overline{u^2}_{yy}$

$\overline{w^2}$: $\varepsilon \sim \nu \overline{w^2}_{yy}$

$\overline{v^2}$: $\overline{p v}_y \sim \Pi_{22} \rightarrow \Pi_{33}$

$\overline{v^2}$ and $\overline{w^2}$: $\overline{p v}_y|_{\overline{v^2}} \text{ near wall} \rightarrow \Pi_{33}$

However, net effect $\overline{p v}_y$ and Π_{22} small and mostly cancel.

$\overline{w^2}$: losses due to ε near wall balanced by $\nu \overline{w^2}_{yy}$

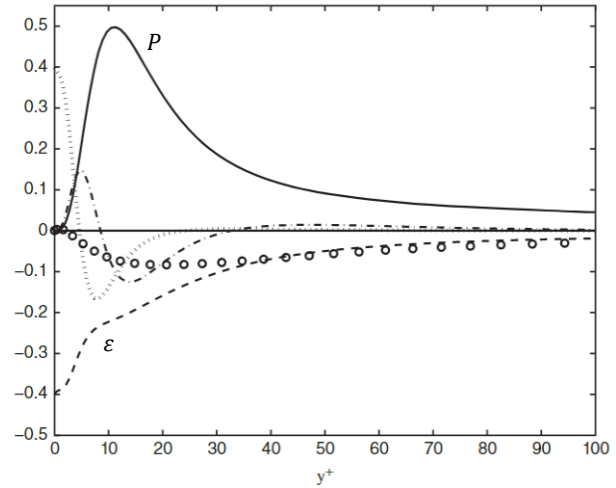


Figure 7.11 $\overline{u^2}$ budget in channel flow for $R_\tau = 5186$ [10]. —, production; ---, dissipation; o, pressure strain; ···, viscous diffusion; - · - ·, turbulent transport.

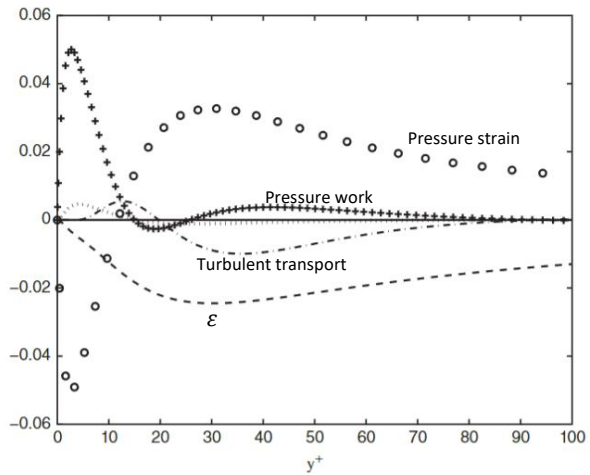


Figure 7.12 $\overline{v^2}$ budget in channel flow for $R_\tau = 5186$ [10]. ---, dissipation; o, pressure strain; +, pressure work; ···, viscous diffusion; - · - ·, turbulent transport.

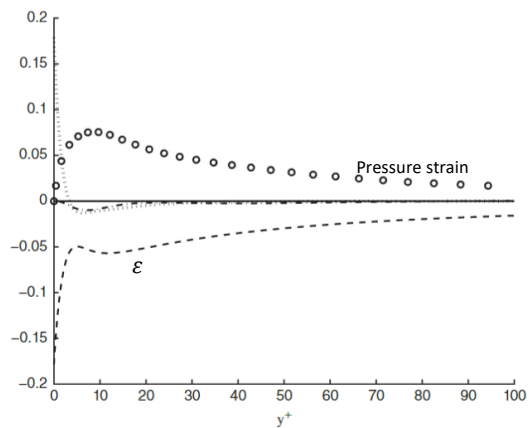


Figure 7.13 $\overline{w^2}$ budget in channel flow for $R_\tau = 5186$ [10]. ---, dissipation; o, pressure strain; ···, viscous diffusion; - · - ·, turbulent transport.

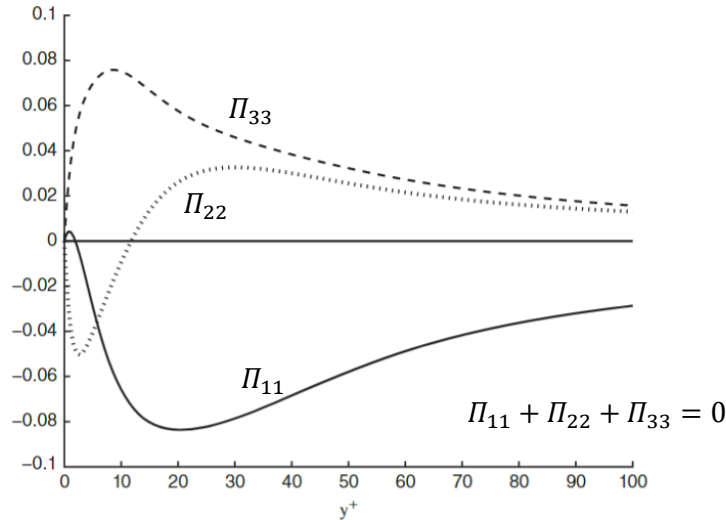


Figure 7.14 Pressure-strain term in normal Reynolds stress equations at $R_\tau = 5186$ [10]: —, Π_{11} ; ···, Π_{22} ; ---, Π_{33} .

Viscous and turbulent transport result in spatial redistribution.

Consider now Reynolds \overline{uv} balance:

$$0 = \underbrace{-\overline{v^2} \frac{d\overline{U}}{dy}}_{\boxed{1}} - \underbrace{\varepsilon_{12}}_{\boxed{2}} + \underbrace{\Pi_{12}}_{\boxed{3}} - \underbrace{\frac{d\overline{uv^2}}{dy}}_{\boxed{4}} - \underbrace{\frac{1}{\rho} \frac{d\overline{p}u}{dy}}_{\boxed{5}} + \underbrace{v \frac{d^2\overline{uv}}{dy^2}}_{\boxed{6}}$$

- 1) Production
- 2) Dissipation: small
- 3) Pressure strain
- 4) Turbulent transport
- 5) Pressure work
- 6) Viscous diffusion: small

4) and 5) cancel.

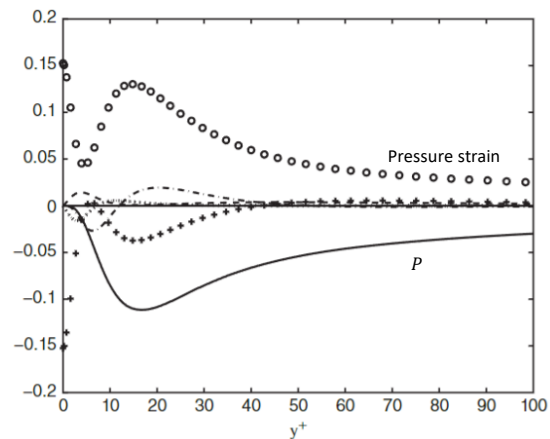


Figure 7.15 \overline{uv} budget in channel flow for $R_\tau = 5186$ [10]. —, production; ---, dissipation; o, pressure strain; +, pressure work; ···, viscous diffusion; - · -, turbulent transport.

$\overline{uv} < 0$ lower channel produced by 1)

Mostly balance of P and $\Pi_{12} \rightarrow$ important to model it correctly.

2) and 6) small $\rightarrow \overline{uv} \neq f(\nu)$

3) and 5) nearly cancel near wall \rightarrow can be combined for modeling.

Enstrophy budget

$$\zeta = \overline{\omega_1^2} + \overline{\omega_2^2} + \overline{\omega_3^2}$$

$\overline{\omega_1^2} \sim \overline{\omega_2^2} \sim \overline{\omega_3^2}$ away from wall.

$$\overline{\omega_1^2}(0) = \overline{w_y^2}(0)$$

$$\overline{\omega_2^2}(0) = 0$$

$$\overline{\omega_3^2}(0) = \overline{u_y^2}(0) \gg \overline{w_y^2}(0)$$

Also associated $\overline{\Omega_3} = -\overline{U_y}$ near wall Fig. 7.3.

Peak in $\overline{\omega_1^2}(0)$ due to spanwise motions near wall.

Anisotropy $10 \leq y^+ \leq 30$: complex physics buffer layer

$$\frac{\varepsilon}{\nu} = \zeta + \frac{d^2 \overline{v^2}}{dy^2}$$

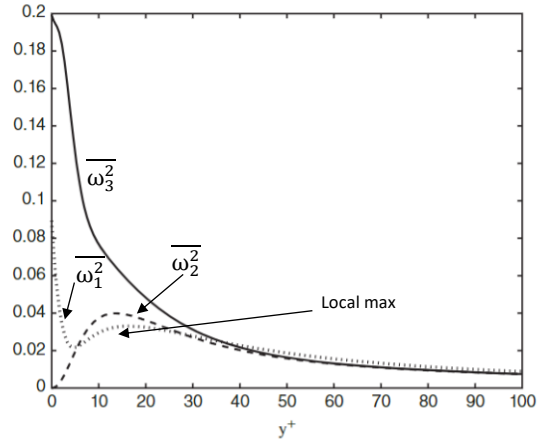


Figure 7.16 Comparison of the enstrophy components in channel flow at $Re = 5186$ [10]: $\cdots, \overline{\omega_1^2}$; $---$, $\overline{\omega_2^2}$; $-$, $\overline{\omega_3^2}$.

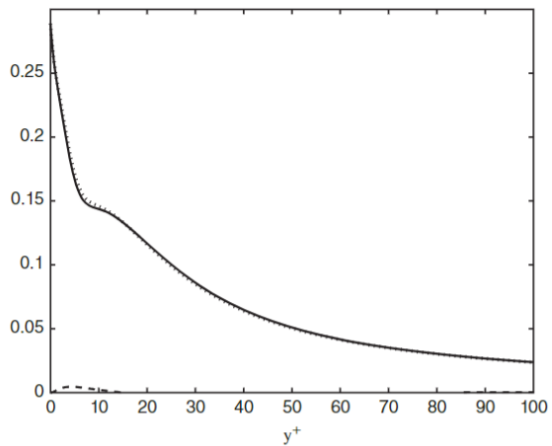
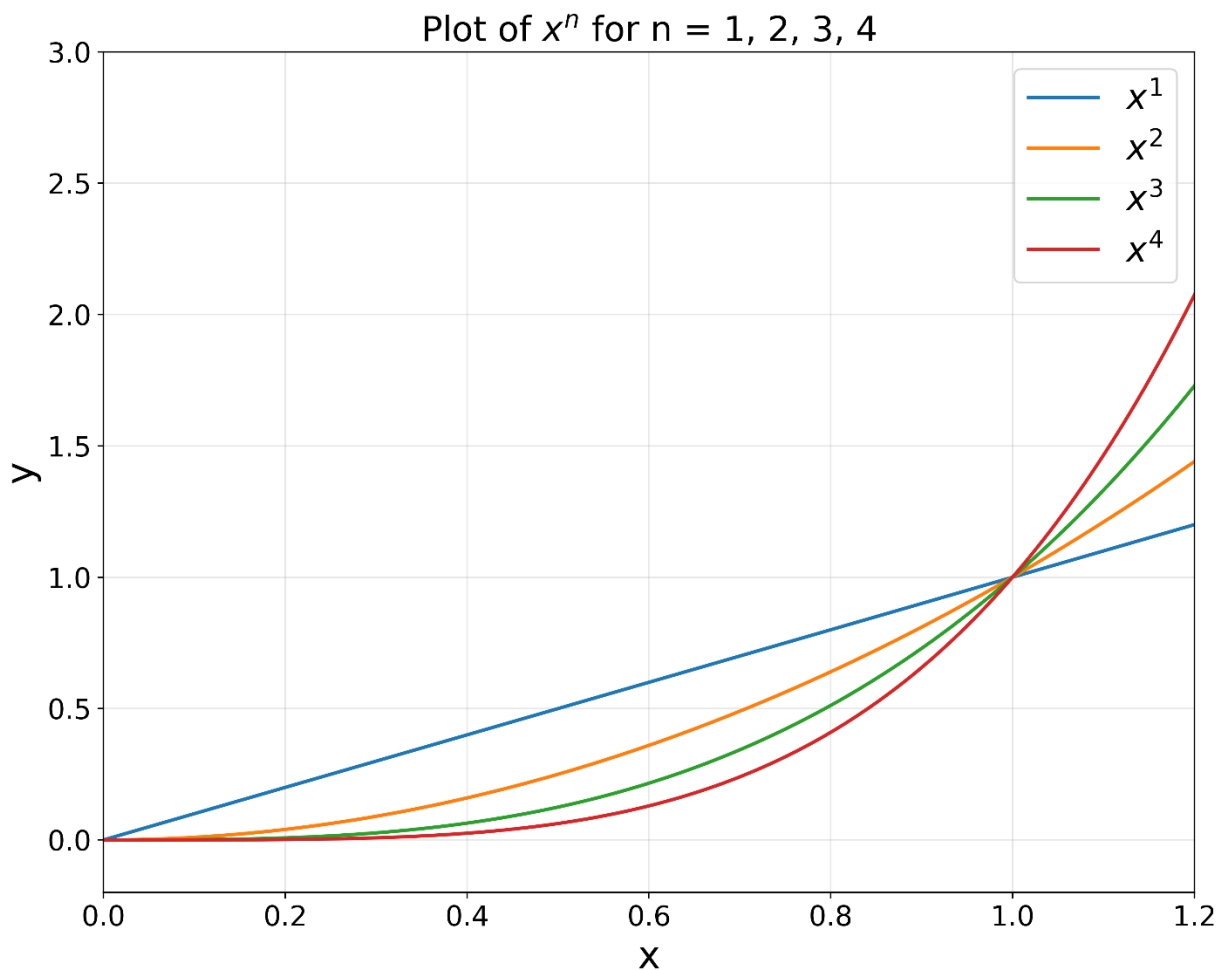


Figure 7.17 Evaluation of the terms in Eq. (7.54) in channel flow with $Re = 5186$ [10]: $\cdots, -\varepsilon^+$; $-$, ζ^+ ; $---$, $d^2 \overline{v^2} / dy^{+2}$.

Mixing Length and Law of the Wall

Taylor Series near $y = 0$ shows $\langle uv \rangle \sim y^3$, whereas mixing length theory for sublayer shows $\frac{-\langle uv \rangle}{u_\tau} \sim l_m^{+2} \sim y^{+2}$ (Pope Ex. 7.19). Fundamental properties log law region (1)-(3) show in log-law region show $l_m^+ = \kappa y^+$ (Pope pg. 289). Thus, the mixing length needs damping to properly merge between the sub and log layers via the buffer layer. One approach is Spalding, as already discussed another is Van Dreist, which leads to $\frac{-\langle uv \rangle}{u_\tau} \sim y^{+4}$ (Pope Ex. 7.19).



EXERCISE

- 7.19 Show that, according to the mixing-length hypothesis, very close to the wall ($y^+ \ll 1$) the Reynolds shear stress is

$$-\frac{\langle uv \rangle}{u_\tau^2} \approx (\ell_m^+)^2. \quad (7.146)$$

Show that the van Driest specification (Eq. (7.145)) yields

$$-\frac{\langle uv \rangle}{u_\tau^2} \approx \left(\frac{\kappa}{A^+}\right)^2 y^{+4}. \quad (7.147)$$

Contrast this result to the correct dependence of $\langle uv \rangle$ on y (for very small y), Eq. (7.63).

According to the mixing length hypothesis, as shown in Equation (7.87) of text, the eddy viscosity is,

$$\nu_T = \ell_m^2 \left| \frac{d\langle U \rangle}{dy} \right|, \quad (1)$$

where ℓ_m is the mixing length, $\langle U \rangle$ the time-averaged streamwise velocity, and y the wall-normal coordinate. It follows then that the Reynolds stress, $-\langle uv \rangle$, is approximated as,

$$-\langle uv \rangle = \nu_T \frac{d\langle U \rangle}{dy} = \ell_m^2 \left| \frac{d\langle U \rangle}{dy} \right| \frac{d\langle U \rangle}{dy}. \quad (2)$$

The expression $d\langle U \rangle/dy$ can be rewritten as,

$$\begin{aligned} \frac{d\langle U \rangle}{dy} &= \frac{d\langle U \rangle}{dy} \frac{u_\tau \delta_\nu}{u_\tau \delta_\nu} \\ &= \frac{d(\langle U \rangle / u_\tau)}{d(y / \delta_\nu)} \frac{u_\tau}{\delta_\nu} \\ &= \frac{du^+}{dy^+} \frac{u_\tau}{\delta_\nu} \\ &= 1 \cdot \frac{u_\tau}{\delta_\nu} = \frac{u_\tau^2}{\nu}. \end{aligned} \quad (3)$$

In the foregoing equation, u_τ is the friction velocity and δ_ν is the viscous lengthscale. Also, $du^+/dy^+ = 1$ for $y^+ \ll 1$ in the viscous sublayer; see Equation (7.40) of text. With the expression for $d\langle U \rangle/dy$ in Equation (3), Equation (2) normalized by the square of u_τ can be reexpressed as,

$$\begin{aligned} \frac{-\langle uv \rangle}{u_\tau^2} &= \ell_m^2 \left| \frac{u_\tau^2}{\nu} \right| \frac{u_\tau^2}{\nu} \frac{1}{u_\tau^2} \\ &= \ell_m^2 \frac{u_\tau^2}{\nu^2} = \frac{\ell_m^2}{\delta_\nu^2} = (\ell_m^+)^2. \end{aligned} \quad (4)$$

In Equation (4), $\ell_m^+ = \ell_m/\delta_\nu$ is the mix-length in viscous scales. And the shear stress would be positive with the assumption of attached flow.

The second part of the question is based on the van Driest approximation, where

$$\ell_m^+ = \kappa y^+ [1 - \exp(-y^+/A^+)]. \quad (5)$$

Using the result from Equation (4),

$$(\ell_m^+)^2 = \kappa^2 (y^+)^2 [1 - 2 \exp(-y^+/A^+) + \exp(-2y^+/A^+)]. \quad (6)$$

Recall the Taylor series expansion for e^x as,

$$e^x = 1 + x + \frac{x^2}{2!} + \frac{x^3}{3!} + \frac{x^4}{4!} + \mathcal{O}(x^5). \quad (7)$$

Therefore, Equation (6) can be rewritten as,

$$\begin{aligned} (\ell_m^+)^2 = \kappa^2 (y^+)^2 & \left\{ 1 - 2 \left[1 - \frac{y^+}{A^+} + \frac{1}{2!} \left(\frac{y^+}{A^+} \right)^2 + \mathcal{O} \left(\left(\frac{y^+}{A^+} \right)^3 \right) \right] \right. \\ & \left. + \left(1 - 2 \frac{y^+}{A^+} + \frac{1}{2!} \left(\frac{2y^+}{A^+} \right)^2 + \mathcal{O} \left(\left(\frac{y^+}{A^+} \right)^3 \right) \right) \right\}. \quad (8) \end{aligned}$$

Simplifying the above expression,

$$(\ell_m^+)^2 = \kappa^2 (y^+)^2 \left[- \left(\frac{y^+}{A^+} \right)^2 + 2 \left(\frac{y^+}{A^+} \right)^2 + \mathcal{O} \left(\left(\frac{y^+}{A^+} \right)^3 \right) \right]. \quad (9)$$

Neglecting higher order terms, the desired form of the solution is,

$$(\ell_m^+)^2 = \kappa^2 (y^+)^2 \left(\frac{y^+}{A^+} \right)^2. \quad (10)$$

Finally,

$$\frac{-\langle uv \rangle}{u_\tau^2} = (\ell_m^+)^2 = \frac{\kappa^2}{(A^+)^2} (y^+)^4. \quad (11)$$

The correct expression for the near-wall Reynolds shear stress is, according to Equation (7.63),

$$\langle uv \rangle = \langle b_1 c_3 \rangle y^3 + \mathcal{O}(y^4),$$

where b_1 and c_3 are constants. Evidently, the form of the near-wall Reynolds stresses deduced based on boundary conditions suggests an asymptotic behavior similar to a third order polynomial, which differs from the polynomial derived based on the van Driest approximation. It seems that the van Driest function for mixing length is not exactly correct for $y^+ \ll 1$.

$$(1) \frac{d\bar{u}}{dy} = \frac{1}{\kappa y} \quad \text{or} \quad \frac{d\bar{u}}{dy} = \frac{u_*}{\kappa y} = S$$

$$(2) P/\varepsilon \approx 1 \quad u_* = \sqrt{\frac{\varepsilon u_*}{\rho}}$$

$$(3) -\langle u'v' \rangle / \varepsilon \approx 0.3$$

Fundamental property (1) log-law region:

$$S = \bar{\sigma}_y \\ = u_* / \kappa y$$

$$S_2 / \varepsilon = \left| \frac{u_*}{\langle u'v' \rangle} \right| \frac{P}{\varepsilon} \approx 3$$

$$P = -\langle u'v' \rangle S$$

$$S = P / -\langle u'v' \rangle$$

$$S_2 / \varepsilon = \left| \frac{P}{-\langle u'v' \rangle} \right| \frac{P}{\varepsilon} \\ \approx 3^{-1}$$

$$LHS = S^{-1} P \frac{\langle u'v' \rangle^{-1}}{\varepsilon^{3/2}}$$

$$= \frac{\varepsilon^{3/2}}{S} S^{-1} P = \frac{P}{S^2 \varepsilon}$$

$$L = \varepsilon^{3/2} / \varepsilon = \kappa \kappa y \frac{|\langle u'v' \rangle|^{1/2} \left(\frac{P}{\varepsilon} \right)}{u_*} \left| \frac{\langle u'v' \rangle}{\varepsilon} \right|^{-3/2}$$

For high Re , in log-law region $\langle u'v' \rangle / u_* \sim \text{constant}$
such that

$$L = \kappa y \quad \langle L = \kappa \left(\frac{P}{\varepsilon} \right) \left| \frac{\langle u'v' \rangle}{\varepsilon} \right|^{-3/2} \approx 2.5$$

Note S, P , at $\varepsilon = P$ vary y^{-1} , whereas L & $\bar{\sigma} = \frac{1}{\kappa} \frac{u_*}{y}$ vary y .
 $\frac{u_*}{\varepsilon} = \frac{S^2}{\varepsilon} = S$
then we have

$$-\langle u'v' \rangle = u_*^2 \ln \bar{\sigma}_y \\ = \frac{1}{\kappa} u_*^2 \ln \bar{\sigma}_y$$

$$-\langle u'v' \rangle = \frac{1}{\kappa} \bar{\sigma}_y^2 \\ = \ln^2 |\bar{\sigma}_y| \bar{\sigma}_y$$

$$v_T = u_*^2 \ln = |\langle u'v' \rangle|^{1/2} \ln$$

one specifies the other determines v_T

$$|\langle u'v' \rangle| = \frac{1}{\kappa} u_*^2 \ln^2 |\bar{\sigma}_y| \\ u_*^2 = \frac{1}{\kappa} \frac{v_T^2}{\ln^2}$$

Assume $u_*^2 = |\langle u'v' \rangle|^{1/2}$

$$= \ln^2 |\bar{\sigma}_y| \quad \text{abs value}$$

for validity

Again in log-law region $-\langle u'v' \rangle \sim u_*^2$ upper/lower

$$u_*^2 = \ln^2 u_*^2 \\ \ln^2 = \ln^2$$

$\bar{\sigma}_y \sim u_* / \kappa y$; consequently, $u_*^2 = u_*^2$ channel

$$\ln = \kappa y$$

$$\ln = \kappa y \quad \text{here } L \text{ is } \propto y$$

In summary $v_T = u_*^2 \ln = \ln^2 |\bar{\sigma}_y|$. In log-law region, $\ln \propto y$, where u_* reads simply for sub & upper layer & additional contributions outer layer.

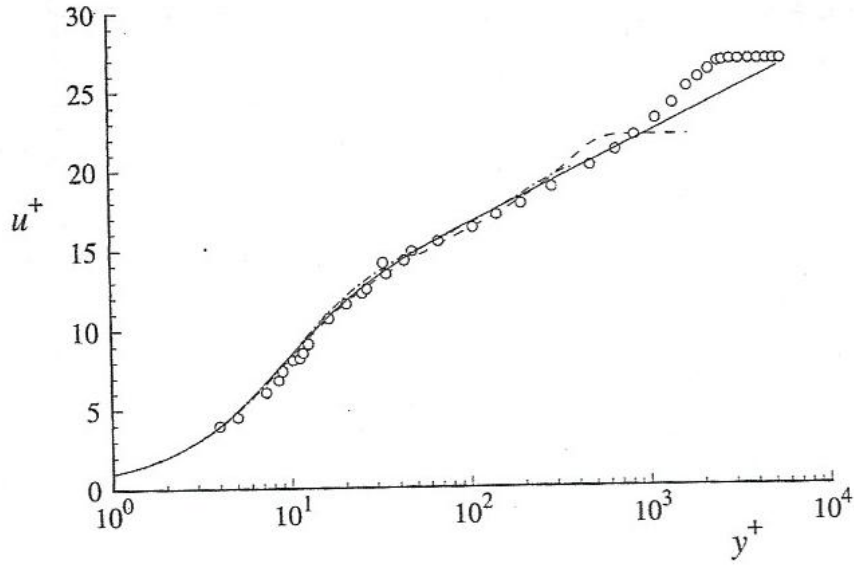


Fig. 7.27. Mean velocity profiles in wall units. Circles, boundary-layer experiments of Klebanoff (1954), $Re_\theta = 8,000$; dashed line, boundary-layer DNS of Spalart (1988), $Re_\theta = 1,410$; dot-dashed line, channel flow DNS of Kim *et al.* (1987), $Re = 13,750$; solid line, van Driest's law of the wall, Eqs. (7.144)–(7.145).

Using the mixing length hypothesis for a boundary layer with zero pressure gradient such that $\partial \bar{U} / \partial y > 0$:

$$\frac{\tau(y)}{\rho} = \nu \frac{\partial \bar{U}}{\partial y} + \nu_t \frac{\partial \bar{U}}{\partial y} = \nu \frac{\partial \bar{U}}{\partial y} + l_m^2 \left(\frac{\partial \bar{U}}{\partial y} \right)^2 \quad (1)$$

where $-\overline{u'v'} = \nu_t \frac{\partial \bar{U}}{\partial y}$ and $\nu_t = l_m^2 \frac{\partial \bar{U}}{\partial y}$

(1) Derive the law of the wall in the sub layer assuming $\nu_t \frac{\partial \bar{U}}{\partial y} = 0$.

(2) Derive the overlap layer log law assuming $\nu \frac{\partial \bar{U}}{\partial y} = 0$ and $l_m^+ = \kappa y^+$. $l_m^+ = \frac{l_m}{\delta_v} = l_m u_\tau / \nu$ ($\delta_v = \nu / u_\tau =$ viscous length scale and $u_\tau = \sqrt{\tau_w / \rho}$ in the friction velocity).

(3) Derive an approximate sub + buffer layer formula assuming $l_m^+ = \alpha_0^2 y^+ + (1 + \alpha_0^2 y^{+2})^{1/2}$ when $\delta_v = \nu/u_\tau =$ viscous length scale and $u_\tau = \sqrt{\tau_w/\rho}$ in the friction velocity and $\frac{\tau}{\tau_w} = 1$; compare with $u^+ = 5 \ln y^+ - 3.05$.

(4) Compare the results with van Driest $l_m^+ = \kappa y^+ \left[1 - \exp\left(\frac{-y^+}{A^+}\right)\right]$ $A^+ = 26$ and Spalding $y^+ = u^+ + e^{-\kappa B} [e^z - 1 - z - z^2/2 - z^3/6]$. $z = \kappa u^+$ and $B = 5.3$ formulas valid in the sub, buffer, and log layers

Approach: nondimensionalize $\frac{\tau(y)}{\rho}$ equation (1) using $y^+ = y u_\tau / \nu$ and $u^+ = \bar{U}/u_\tau$ and solve resulting quadratic equation for $\frac{\partial u^+}{\partial y^+}$, which can then be integrated according to (1) – (4) specifications for ν_t, ν and l_m^+ ; and compared with the Spalding formula. Note that $\alpha_0 = 0.3, \kappa = 0.41, B = 5.3$

Results

$$\frac{\tau}{\tau_w} = \frac{\partial u^+}{\partial y^+} + \left(l_m^+ \frac{\partial u^+}{\partial y^+} \right)^2$$

$$\frac{\partial u^+}{\partial y^+} = \frac{2\tau/\tau_w}{1 + [1 + 4(\tau/\tau_w)l_m^{+2}]^{1/2}} \quad (\text{alternate form solution quadratic equation})$$

In the inner layer the ratio $\frac{\tau}{\tau_w} \approx 1$ so that the law of the wall is obtained in terms of the mixing length:

$$u^+ = f_w(y^+) = \int_0^{y^+} \frac{2dy^+}{1 + [1 + 4l_m^{+2}]^{1/2}} dy^+$$

(1)

$$1 = \frac{\partial u^+}{\partial y^+} \rightarrow u^+ = y^+.$$

(2)

$$1 = (\kappa y^+)^2 \left(\frac{\partial u^+}{\partial y^+} \right)^2 \rightarrow \frac{\partial u^+}{\partial y^+} = \frac{1}{\kappa y^+}$$

$$u^+ = \frac{1}{\kappa} \ln(y^+) + B$$

(3)

$$\begin{aligned} 1+4l^{+2} &= 1 + 4[\alpha_0^2 y^+ + (1 + \alpha_0^4 y^{+2})^{1/2}]^2 = 1 + 4\alpha_0^4 y^{+2} (1 + \alpha_0^4 y^{+2}) \\ &= 1 + 4\alpha_0^4 y^{+2} + 4\alpha_0^8 y^{+4} \end{aligned}$$

$$u^+ = 2 \int_0^{y^+} \frac{dy^+}{2 + 2\alpha_0^4 y^{+2}} = \int_0^{y^+} \frac{dy^+}{1 + \alpha_0^4 y^{+2}}$$

$$A = \alpha_0^2 y^+ \quad \frac{dA}{dy^+} = \alpha_0^2 \quad dy^+ = \frac{1}{\alpha_0^2} dA$$

$$\rightarrow \int_0^{y^+} \frac{dy^+}{1 + \alpha_0^4 y^{+2}} = \frac{1}{\alpha_0^2} \int_0^{\alpha_0^2 y^+} \frac{dA}{1 + A^2}$$

$$\rightarrow \frac{1}{\alpha_0^2} \int_0^{\alpha_0^2 y^+} \frac{dA}{1 + A^2} = \frac{1}{\alpha_0^2} [\tan^{-1}(A)]_0^{\alpha_0^2 y^+}$$

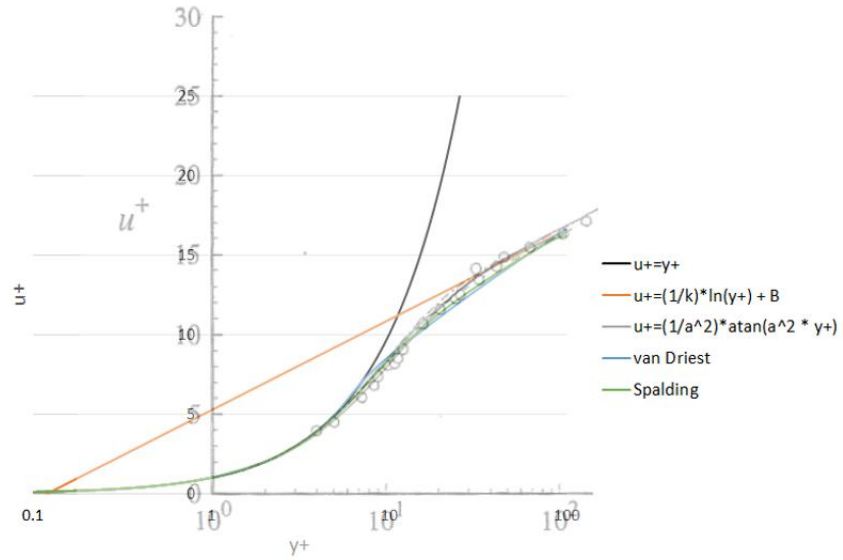
$$\therefore u^+ = \frac{1}{\alpha_0^2} \tan^{-1}(\alpha_0^2 y^+)$$

(4)

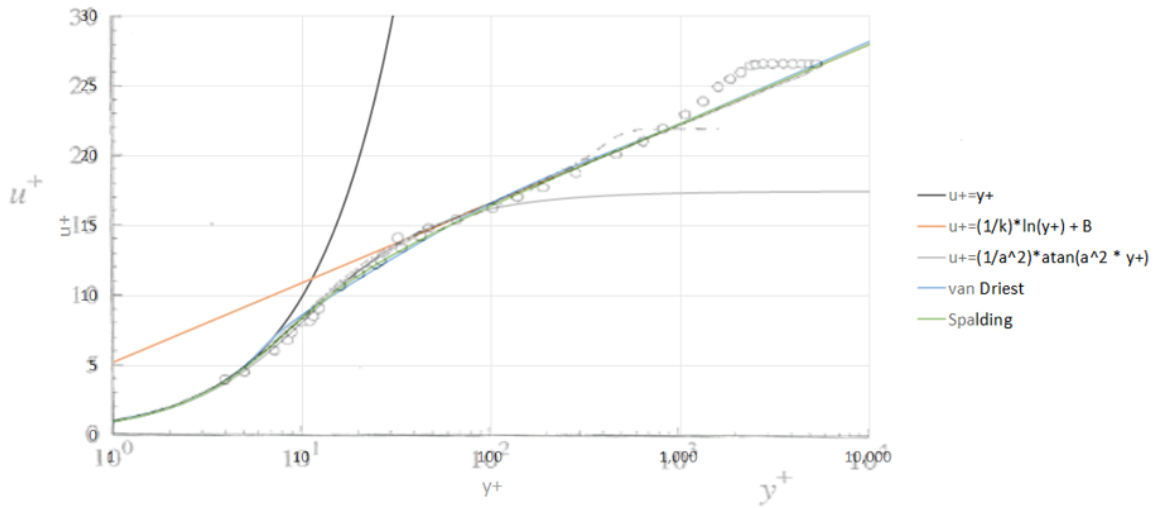
Van Driest:
$$u^+ = \int_0^{y^+} \frac{2dy^+}{1 + [1 + 4\kappa^2 y^{+2} \{1 - e^{(-y^+/A^+)}\}]^2}^{1/2}$$

Spalding:
$$y^+ = u^+ + e^{-\kappa B} [e^Z - 1 - Z - Z^2/2 - Z^3/6], Z = \kappa u^+$$

The latter is purely algebraic, but implicit in u^+ , while the former may be integrated numerically, e.g., Runge-Kutta. Both provide good fits to the data; however, the Van Driest is more flexible as it may be made to fit other conditions such as pressure gradient, blowing/suction, roughness, etc. by changing the value of the damping coefficient



Expanded y^+ range up to 10^4 and added other data set including experiment result (Klebanoff. 1954)



Mean velocity profiles in wall units. Circles, boundary-layer experiments of Klebanoff (1954), $Re_\theta = 8,000$; dashed line, boundary-layer DNS of Spalart (1988), $Re_\theta = 1,410$; dot-dashed line, channel flow DNS of Kim *et al.* (1987), $Re = 13,750$; solid line, van Driest's law of the wall, Eqs. (7.144)–(7.145).

Appendix A.2

$\underline{U}(0) = 0$ determines how $\langle u_i u_j \rangle$ depend from zero for small y . For fixed $x, z, t \neq 0$
Small y TS for \underline{u} :

$$u = a_1 + b_1 y + c_1 y^2 + \dots$$

$$v = a_2 + b_2 y + c_2 y^2 + \dots$$

$$w = a_3 + b_3 y + c_3 y^2 + \dots$$

Coefficients are

zero mean

random variables

at for fully

developed channel

$$\text{no slip: } a_1 = a_2 = a_3 = 0$$

$$u_x = v_y = 0 \Rightarrow v_y = 0$$

flow statistically

ie $b_2 = 0$ independent x, z, t

$b_2 = 0 \Rightarrow$ Z component flow close to surface

$\langle u_i u_j \rangle$ obtained by taking means of products of TS:

$$\langle u^2 \rangle = \langle b_1^2 \rangle y^2 + \dots$$

$$\langle v^2 \rangle = \langle c_2^2 \rangle y^4 + \dots$$

$$\langle w^2 \rangle = \langle b_3^2 \rangle y^2 + \dots$$

$$\langle uv \rangle = \langle b_1 c_2 \rangle y^3 + \dots$$

$\langle u^2 \rangle, \langle w^2 \rangle, \dots$ increase as y^2 , whereas

$\langle uv \rangle$ & $\langle v^2 \rangle$ increase more slowly

ie y^3 & y^4 , respectively.

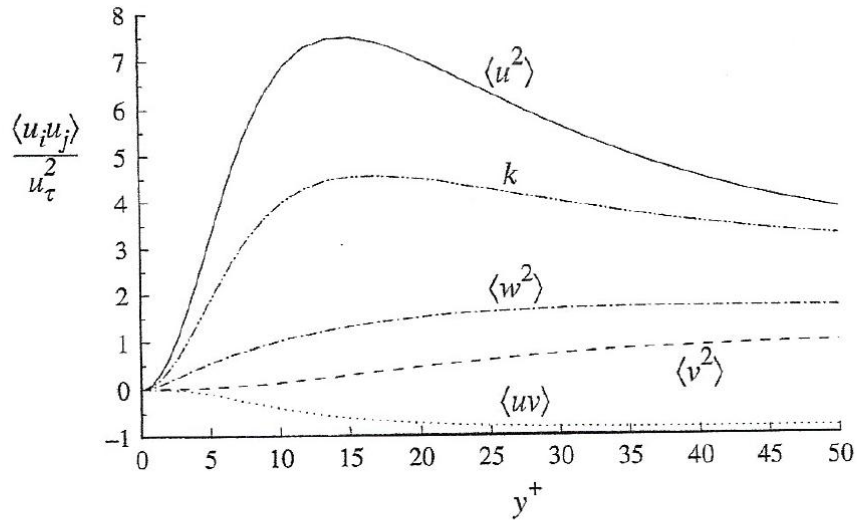


Fig. 7.17. Profiles of Reynolds stresses and kinetic energy normalized by the friction velocity in the viscous wall region of turbulent channel flow: DNS data of Kim *et al.* (1987). $Re = 13,750$.

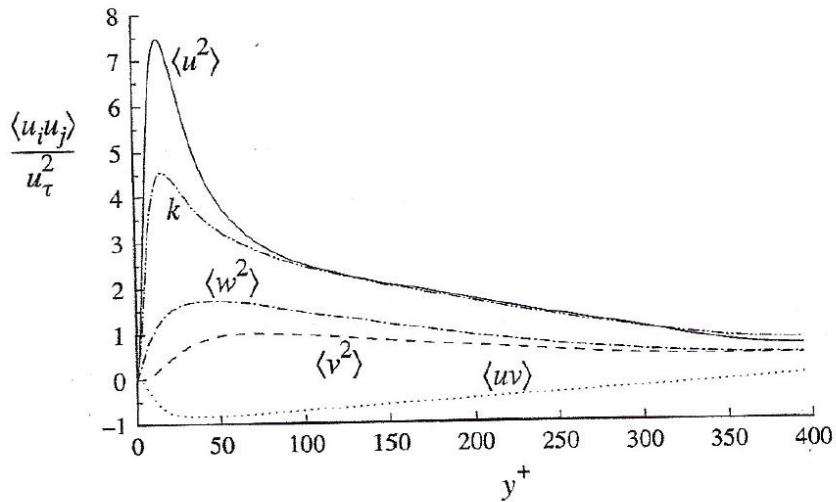


Fig. 7.14. Reynolds stresses and kinetic energy normalized by the friction velocity against y^+ from DNS of channel flow at $Re = 13,750$ (Kim *et al.* 1987).

Appendix A.2

BRIEF NOTES

References

- 1 K.-T. Yang, "Possible Similarity Solutions for Laminar Free Convection on Vertical Plates and Cylinders," *JOURNAL OF APPLIED MECHANICS*, vol. 27, TRANS. ASME, vol. 82, Series E, 1960, pp. 230-236. See also discussion of this paper in March, 1961, issue of the *JOURNAL OF APPLIED MECHANICS*, pp. 153-154.
- 2 R. Eichhorn, "The Effect of Mass Transfer on Free Convection," *Journal of Heat Transfer*—TRANS. ASME, vol. 82, Series C, 1960, pp. 260-263.
- 3 A. S. Gupta, "Steady and Transient Free Convection of an Electrically Conducting Fluid From a Vertical Plate in the Presence of a Magnetic Field," *Applied Science Research*, Section A, vol. 9, 1960, pp. 319-333.

A Single Formula for the "Law of the Wall"

D. B. SPALDING¹

Summary

It is shown that experimental velocity distributions may be well fitted, in the laminar sublayer, the transition region, and the turbulent core, by the formula:

$$y^+ = u^+ + 0.1108\{e^{0.4u^+} - 1 - 0.4u^+ - (0.4u^+)^2/2! - (0.4u^+)^3/3! - (0.4u^+)^4/4!\}$$

Omission of the $(0.4u^+)^4$ term gives an equally good fit. The corresponding expressions for the ratio of turbulent shear stress to total shear stress agree with the measurements of Laufer [8]² quite closely.

Nomenclature

- u = time-mean velocity of fluid in x -direction
- u^+ = $u\sqrt{\rho/\tau}$
- x = distance along the wall in the direction of flow
- y = distance from the wall
- y^+ = $y\sqrt{\tau\rho/\mu_{\text{molecular}}}$
- ϵ^+ = $\mu_{\text{total}}/\mu_{\text{molecular}}$
- $\mu_{\text{molecular}}$ = absolute viscosity of fluid in laminar motion
- μ_{total} = ratio of shear stress to gradient of time-mean velocity
- μ_{turb} = $\mu_{\text{total}} - \mu_{\text{molecular}}$
- ρ = density of fluid
- ϕ = density of fluid divided by density of fluid adjacent to wall
- τ = shear stress in fluid, assumed independent of y

Introduction

Purpose of note. Numerous formulas have been proposed to describe the universal turbulent velocity profile, called by Coles [1] the "law of the wall." The present note discloses a new formula which is valid over the whole range of dimensionless distance y^+ .³ The new formula has a form which, on the one hand, permits analytical determination of several important boundary-layer parameters, and, on the other, may provide the vantage point for a new look at the theory of the turbulent boundary layer. These matters are only touched on briefly in the following.

The universal turbulent velocity profile. Prandtl's [12] postulate, that the velocity in the neighborhood of a wall should obey the relation:

¹ Professor of Heat Transfer, Department of Mechanical Engineering, Imperial College of Science and Technology, London, England. Manuscript received by ASME Applied Mechanics Division, March 8, 1961.

² Numbers in brackets indicate References at end of Note.

³ See Nomenclature at beginning of Note.

$$u^+ = u^+(y^+) \quad (1)$$

has been confirmed experimentally by Nikuradse [10], and subsequently by many other authors.

The experimental relation has been described analytically in various ways, some of which are listed in Table 1. It will be

Table 1 Formulas for the "law of the wall"^a

Author	Range of validity	Formulas
Prandtl [11] ^b	$0 \leq y^+ < 11.5$	$u^+ = y^+$
Taylor [18] ^c	$11.5 \leq y^+ < 30$	$u^+ = 2.5 \ln y^+ + 5.5$
von Karman [7]	$0 \leq y^+ < 5$	$u^+ = y^+$
	$5 \leq y^+ < 30$	$u^+ = 5 \ln y^+ - 3.05$
Reichardt [15]	$30 \leq y^+$	$u^+ = 2.5 \ln y^+ + 5.5$
	$0 \leq y^+$	$u^+ = 2.5 \ln(1 + 0.4y^+) + 7.8\{1 - e^{-y^+/11}\} - (y^+/11)e^{-0.33y^+}$
Deissler [2]	$0 \leq y^+ < 26$	$u^+ = \int_0^{y^+} \frac{dy^+}{1 + n^2 u^+ y^+ (1 - e^{-n^2 u^+ y^+})}$ $n = 0.124$
	$26 \leq y^+$	$u^+ = 2.78 \ln y^+ + 3.8$
van Driest [19]	$0 \leq y^+$	$u^+ = \int_0^{y^+} \frac{dy^+}{2dy^+}$
	$1 + \{1 + 0.64y^{+2}[1 - \exp(-y^+/26)]^2\}^{1/4}$	
Rannie [13]	$0 \leq y^+ < 27.5$	$u^+ = 14.54 \tan h(0.0688y^+)$
	$27.5 \leq y^+$	$u^+ = 2.5 \ln y^+ + 5.5$

^a See also Hofmann [5], Reichardt [14], Rotta [16], Miles [9], Elrod [3], and Frank-Kamenetsky [21].

^b These authors did not, at the dates in question, state the formulas attributed to them in the table. However, they did introduce the idea of a sharp division between a laminar sublayer and a fully turbulent core; when compared with experimental data, this idea leads directly to the formulas given.

noted that all the authors mentioned, except Reichardt [15] and van Driest [19], have found it necessary to use at least two expressions, valid for different ranges of y^+ , in order to describe the profile adequately.

The problem. A single formula, expressing the $u^+(y^+)$ relation over the whole range of the variables, is both more satisfying aesthetically and more convenient practically than the two-point formulas of Table 1. However, Reichardt's formula is rather complex in form, whereas van Driest's involves a quadrature requiring numerical evaluation. There is need for a simpler, easily evaluated formula.

Such a formula would preferably fit the experimental data closely, contain sufficient adjustable constants to permit modification in the light of new experimental data, and have an analytical form permitting easy integration of the various functions of the velocity distribution which arise in, for example, the theory of heat transfer through a turbulent boundary layer.

Looked at mathematically, our problem is to establish a formula which:

- (i) passes through the point: $y^+ = 0, u^+ = 0$;
- (ii) is tangential at this point to: $u^+ = y^+$;
- (iii) is asymptotic at large y^+ to:⁴

$$u^+ = 2.5 \ln y^+ + 5.5 \quad (2)$$

- (iv) fits the experimental points at intermediate y^+ values.

⁴ Here the most popular constants for the logarithmic velocity profile have been accepted.

BRIEF NOTES

The New "Law of the Wall"

The simplest y^+ (u^+) relation. The previous efforts to find a single formula fitting the foregoing specification u^+ has been sought explicitly in terms of y^+ . There is, however, no need to demand this; a relation giving y^+ explicitly in terms of u^+ is just as good, and indeed may even be better for some purposes.

Once this possibility is recognized, progress can be made swiftly. We now seek a $y^+(u^+)$ relation such that

$$\text{near } u^+ = 0: y^+ = u^+ \quad (3)$$

$$\text{and at large } u^+: y^+ = 0.1108e^{0.4u^+} \quad (4)$$

the latter equation being derived directly from equation (2).

The equation which immediately suggests itself is:

$$y^+ = u^+ + 0.1108(e^{0.4u^+} - 1 - 0.4u^+) \quad (5)$$

This satisfies requirements (3) and (4). Does it also fit the experimental data? This can be judged by reference to Fig. 1, which contains the experimental data of Laufer [8]. Evidently, equation (5) fits the data fairly well, but gives values of u^+ which are approximately 10 per cent low when y^+ lies between 10 and 50. Fig. 1 also contains, as broken curves, the asymptotic expressions (2) and (3).

Improved $y^+(u^+)$ relations. If we define a dimensionless "total" (i.e., "molecular plus turbulent" viscosity) ϵ^+ by

$$\epsilon^+ = \mu_{\text{total}}/\mu_{\text{molecular}} \quad (6)$$

then the assumption that the shear stress is independent of distance from the wall, when combined with the definitions of u^+ and y^+ , leads to the relation:

$$\epsilon^+ = \frac{dy^+}{du^+} \quad (7)$$

Equation (5) therefore implies the $\epsilon^+(u^+)$ relation:

$$\begin{aligned} \epsilon^+ &= 1 + 0.4 \times 0.1108(e^{0.4u^+} - 1) \\ &= 1 + 0.04432 \left\{ 0.4u^+ + \frac{(0.4u^+)^2}{2!} + \dots \right\} \end{aligned} \quad (8)$$

Now there are theoretical reasons (Reichardt, [15]; Hinze, [4]) against a growth of ϵ^+ in the wall region with a power of y^+ which is less than 3, if the shear stress varies along the wall, and less than 4 if there is no such variation. Equation (8) satisfies neither requirement.⁶ However, it is easy to see what must be done to the velocity distribution if either of these requirements is to be satisfied: the distribution formula becomes, respectively:

$$y^+ = u^+ + 0.1108 \left\{ e^{0.4u^+} - 1 - 0.4u^+ - \frac{(0.4u^+)^2}{2!} - \frac{(0.4u^+)^3}{3!} \right\} \quad (9)$$

or

$$y^+ = u^+ + 0.1108 \left\{ e^{0.4u^+} - 1 - 0.4u^+ - \frac{(0.4u^+)^2}{2!} - \frac{(0.4u^+)^3}{3!} - \frac{(0.4u^+)^4}{4!} \right\} \quad (10)$$

Curves corresponding to equations (9) and (10) are plotted in Fig. 1. They fit the experimental data rather better than does equation (5), but it is not possible to say which of the two gives the more precise fit. Whether the $(0.4u^+)^4$ term should be included or not will therefore probably have to be decided on other grounds.

⁶Nor, incidentally, do the expressions of Reichardt and van Driest which appear in Table 1.

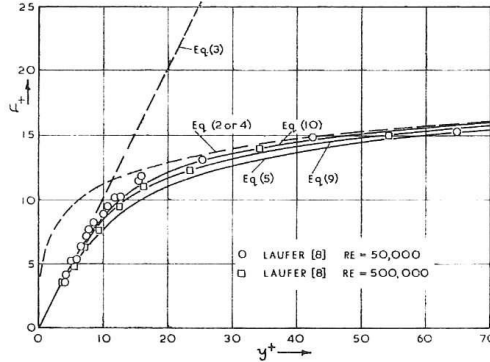


Fig. 1 Experimental data of Laufer [8] for velocity distribution near the wall in turbulent pipe flow, compared with various analytical expressions

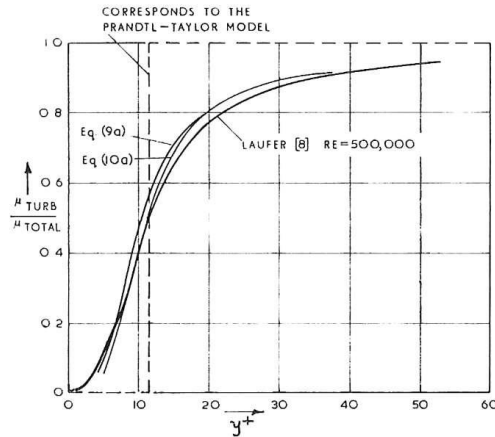


Fig. 2 Experimental data of Laufer on turbulent-stress distribution near the wall in turbulent pipe flow, compared with various analytical expressions

Laufer [8] has also made measurements of the ratio of the turbulent shear stress divided by the total shear stress near the wall. His measurements in a pipe flow, of Reynolds number 500,000, are shown in Fig. 2 as a bold line; y^+ is the abscissa and the viscosity ratio $\mu_{\text{turb}}/\mu_{\text{total}}$ is the ordinate. Also drawn in Fig. 2 are the corresponding relations deduced from equations (9) and (10). These are, respectively:

$$\frac{\mu_{\text{turb}}}{\mu_{\text{total}}} = 1 / \left[1 + 1/0.04432 \left\{ e^{0.4u^+} - 1 - 0.4u^+ - \frac{(0.4u^+)^2}{2!} \right\} \right] \quad (9a)$$

and

$$\frac{\mu_{\text{turb}}}{\mu_{\text{total}}} = 1 / \left[1 + 1/0.04432 \left\{ e^{0.4u^+} - 1 - 0.4u^+ - \frac{(0.4u^+)^2}{2!} - \frac{(0.4u^+)^3}{3!} \right\} \right] \quad (10a)$$

Comparison of these relations with the experimental curves shows that the former equation gives the better fit at low y^+ , while the latter gives the better fit at high y^+ . However, it is probable that both curves can be regarded as equally satisfactory when experimental scatter is taken into account.

Also plotted in Fig. 2, as a broken steplike curve, is the $\mu_{\text{turb}}/\mu_{\text{total}}$ distribution which corresponds to the assumption of a sharp boundary between a laminar sublayer and a fully turbulent outer region. Clearly this gives a very poor representation of the data.

Further possible improvements. Equation (10) fits the requirement that ϵ^+ increases with the fourth power of u^+ , and so of y^+ , close to the wall. However, even if this is correct, there is no reason why the first nonzero term of the expansion should happen to be that which appears in the expansion of $0.1108e^{0.4u^+}$. In other words, it may be that further terms should appear inside the braces of equations (9) and (10) which have the effect of only partially canceling the corresponding terms in the exponential expansion. Discussion of such further developments will be deferred to a later publication.

Discussion

Practical use of the new formula. Fig. 1 shows that equations (9) or (10) can be used to represent the "law of the wall" within the accuracy of the experimental data. Moreover, as just noted, the general form of these equations is sufficiently flexible to accommodate any further modifications of constants which experiment shows to be necessary. Of course, the constants 0.4 and 0.1108 must not be regarded as sacrosanct.

It should also be noted that the form of the equations is very suitable for analytical work involving such expressions as $\int u^+ dy^+$; for this integral can be written as $\int u^+(dy^+/du^+)du^+$, which can be evaluated in closed form, since dy^+/du^+ is easily obtained by differentiating the $y^+(u^+)$ relation. The way is therefore open to the analytical derivation of drag laws, for example, without the approximations which are usually introduced (e.g., "seventh-power" profiles). These possibilities will be elaborated elsewhere. (See, for example, Spalding [17].)

Theoretical implications. Equations (9) and (10) are presented solely as useful interpolation formulas; they are not based on any postulated mechanism of turbulent transport. Nevertheless, they provoke certain questions which it may be profitable to investigate further. Some of these will now be listed.

(i) Does (10), for example, satisfy a differential equation in which u^+ and y^+ appear *only* as differentials?

The answer is readily seen; it is:

$$\frac{d^2y^+}{du^{+5}} = 0.4 \frac{d^2y^+}{du^{+5}} \quad (11)$$

Similarly, equation (5) satisfies the differential equation:

$$\frac{d^2y^+}{du^{+3}} = 0.4 \frac{d^2y^+}{du^{+3}} \quad (12)$$

(ii) Such differential equations are reminiscent of those derived by Prandtl [12] and von Karman [7] as starting points for the logarithmic velocity profile. Can a physical significance be attached to these equations? Could they have been derived by postulation of a physical model followed by dimensional analysis?

(iii) The von Karman differential equation is derived from the consideration that the local "mixing length" must be related to local values of $(\partial u/\partial y)$, $(\partial^2 u/\partial y^2)$, and so forth. Is there any reason why u should have been chosen as dependent and y as independent variable in this analysis, other than the irrelevant one that we happen to perform experiments by fixing the position of the Pitot tube first and then taking the reading? If not, a relation of the mixing length to $(\partial y/\partial u)$, $(\partial^2 y/\partial u^2)$, and so on, is equally valid.

(iv) When the density varies such that density ratio ϕ is a known function of u^+ , is it reasonable to calculate the velocity profile from a suitably modified version of (11)? This would run:

$$\frac{d^2y^+}{du^{+5}} = 0.4\phi(u^+) \frac{d^2u^+}{du^{+5}} \quad (13)$$

which can be evaluated by numerical quadrature without difficulty. This thought might lead to more satisfactory theories of friction and heat transfer in compressible boundary layers. If equation (13) is not as suitable a starting point for analysis as that, for example, of van Driest [20], what is the physical reason for this?

It is not intended to suggest answers to these questions here. They are put forward solely to provoke thought and criticism.

Conclusions

(a) Formulas have been presented [equations (9) and (10)] which represent adequately the experimental data for the universal turbulent velocity profile when the viscosity and density of the fluid are uniform.

(b) The formulas are flexible enough to permit further adjustment of constants in the light of new experimental data, and simple enough in form to permit analytical integration in important cases of interest.

(c) The formulas represent y^+ explicitly in terms of u^+ instead of vice versa. It appears possible that other aspects of turbulent boundary-layer analysis may be profitably re-examined with velocity as the independent variable.

Acknowledgment

The author expresses his gratitude to Prof. J. O. Hinze of Delft, Holland, for his helpful comments on an earlier draft of this Note.

References

- 1 D. Coles, "The Law of the Wake in the Turbulent Boundary Layer," *Journal of Fluid Mechanics*, vol. 1, 1956, pp. 191-226.
- 2 R. G. Deissler, "Analysis of Turbulent Heat Transfer, Mass Transfer and Friction in Smooth Tubes at High Prandtl and Schmidt Numbers," NACA Tech. Rep. 1210, 1955 (supersedes NACA Tech. Note 3145, 1954).
- 3 H. G. Elrod, "Note on the Turbulent Shear Stress Near a Wall," *Journal of the Aeronautical Sciences*, vol. 24, 1957, p. 468.
- 4 J. O. Hinze, "Turbulence," McGraw-Hill Book Company, New York, N. Y., 1959, p. 472.
- 5 E. Hofmann, *Forschung a.d. Geb. Ing.*, vol. 11A, 1940, p. 159.
- 6 T. von Karman, "Mechanische Ähnlichkeit u. Turbulenz," *Nachr. Ges. der Wiss. Göttingen, Math. Phys. Klasse*, vol. 58, 1930.
- 7 T. von Karman, "The Analogy Between Fluid Friction and Heat Transfer," *Trans. ASME*, vol. 61, 1939, pp. 705-710.
- 8 J. Laufer, "The Structure of Turbulence in Fully Developed Pipe Flow," NACA Tech. Rep. 1174, 1954.
- 9 J. W. Miles, *Journal of the Aeronautical Sciences*, vol. 24, 1957, p. 704.
- 10 J. Nikuradse, "Gesetzmässigkeiten der turbulenten Strömung in glatten Röhren," *Forschung a.d. Geb. Ing.*, No. 356, 1932.
- 11 L. Prandtl, "Eine Beziehung zwischen Wärmeaustausch und Strömungswiderstand der Flüssigkeit," *Z. Physik*, vol. 11, 1910, pp. 1072-1078.
- 12 L. Prandtl, "Über die ausgebildete Turbulenz," *Z. für angew. Math. Mech.*, vol. 5, 1925, p. 136.
- 13 W. D. Rannie, "Heat Transfer in Turbulent Shear Flow," *Journal of the Aeronautical Sciences*, vol. 23, 1956, p. 485.
- 14 H. Reichardt, "Die Wärmeübertragung in turbulenten Reibungsschichten," *Z. angew. Math. Mech.*, vol. 20, 1940, p. 297.
- 15 H. Reichardt, "Vollständige Darstellung der turbulenten Geschwindigkeitsverteilung in glatten Leitungen," *Z. angew. Math. Mech.*, vol. 31, 1951, pp. 208-219.
- 16 J. Rotta, *Ing.-Archiv*, vol. 18, 1950, p. 277.
- 17 D. B. Spalding, "Heat Transfer to a Turbulent Stream From a Surface With a Step-Wise Discontinuity in Wall Temperatures," paper to be presented at the joint ASME-I. Mech. E. Heat Transfer Conference, Boulder, Colo., August 28-September 1, 1961.

⁶ Or, of course, less.

BRIEF NOTES

18 G. I. Taylor, "Conditions at the Surface of a Hot Body Exposed to the Wind," Brit. Aero. Res. Comm. R&M No. 272, 1916, p. 423.

19 E. R. van Driest, "On Turbulent Flow Near a Wall," *Journal of the Aeronautical Sciences*, vol. 23, 1956, p. 1007.

20 E. R. van Driest, "Turbulent Boundary Layer in Compressible Fluids," *Journal of the Aeronautical Sciences*, vol. 18, 1951, p. 145.

21 D. A. Frank-Kamenetsky, "Diffusion and Heat Exchange in Chemical Kinetics," Princeton University Press, 1955, p. 184. First published in the USSR, 1947.

On Classical Normal Modes of a Damped Linear System

MORRIS MORDUCHOW¹

IT HAS BEEN essentially shown by Rayleigh [1]² that if the damping matrix of a linear vibrating system is a linear combination of the stiffness and inertia matrices, then the damped system will have principal modes which are exactly the same as those of the undamped system. Caughey [2] has recently developed more general conditions for the existence of classical normal modes with damping, including the above condition as a special case. In both [1] and [2], the analysis is based on the use of normal coordinates. The purpose of this Note is to demonstrate Rayleigh's condition (equation (2) below) in a straightforward manner without the use of normal co-ordinates and hence without assuming a knowledge of the theory associated with transformations to such co-ordinates. This procedure, in addition to being instructive, will also lead to explicit results for the damping factor and natural frequency in any principal mode, and will be seen to yield some interesting implications. Finally, the method of analysis given here will be applied to a vibrating beam with simultaneous internal and external damping.

Let a dynamical system be governed by the equations

$$[m]\{\ddot{h}\} + [c]\{\dot{h}\} + [k]\{h\} = 0 \quad (1)$$

where $[m]$, $[c]$, and $[k]$ are square (inertia, damping, and stiffness, respectively) matrices of order n . Moreover, suppose

$$[c] = a[m] + b[k] \quad (2)$$

where a and b are any constants. To solve equations (1), let

$$\{h\} = \{H\}e^{pt} \quad (3)$$

where $\{H\}$ is independent of the time t , and p is a constant. Then, if equation (2) holds, equation (1) reduces to

$$([m] + \frac{1+bp}{p^2+ap})\{k\}\{H\} = 0 \quad (4)$$

Equation (4) is seen to be the same as the equation for no damping ($a = b = 0$), but with $(1/p^2)$ replaced by $(1+bp)/(p^2+ap)$. Hence the characteristic normalized vectors $\{H\}$ with damping will be the same as those without the damping. Moreover, if in the k th mode without damping $p_k^2 = -\omega_{ko}^2$ (where ω_{ko} denotes the undamped natural frequency in the k th mode), then for the k th mode with damping

$$\frac{1+bp_k}{p_k^2+ap_k} = -\frac{1}{\omega_{ko}^2} \quad (5)$$

Thus

$$p_k = -d_k \pm i\omega_k \quad (6a)$$

¹ Associate Professor of Applied Mathematics, Polytechnic Institute of Brooklyn, Brooklyn, N. Y.

² Numbers in brackets indicate References at end of Note.

Manuscript received by ASME Applied Mechanics Division, March 2, 1961.

where

$$d_k = \frac{a + \omega_{ko}^2 b}{2}, \quad \omega_k = \omega_{ko} \left[1 - \left(\frac{d_k}{\omega_{ko}} \right)^2 \right]^{1/2} \quad (6b)$$

Equations (6a, b) give the damping factor d_k and the natural frequency ω_k for any principal mode with damping when condition (2) holds. In the latter case, in fact, a necessary and sufficient condition for *dynamic stability* of the system is that

$$a + \omega_{ko}^2 b \geq 0 \quad (7)$$

for each undamped natural frequency ω_{ko} . [It is interesting to note that (7) can be satisfied even in cases when either a or b (but not both) is negative. Equations (3) through (6b) are valid whether $[c]$ is positive definite or not.]

Consider, finally, a beam subjected to an external damping load $f(x)\partial Y/\partial t$ and an internal damping load $(g/\omega)\partial/\partial t(EIY''')$ (cf., e.g., [3]) per unit length, where $\partial \equiv \partial/\partial x$. Moreover, suppose $f(x) = cp(x)$, where c is a constant,³ and $\rho(x)$ is the mass per unit length of the beam. Let $Y(x, t) = y(x)e^{pt}$. Then the equation for the free bending vibrations reduces to:

$$(EI(x)y''')'' + \rho(x) \left(\frac{cp + p^2}{1 + \frac{g}{\omega} p} \right) y = 0 \quad (8)$$

Hence the principal mode shapes $y(x)$ will be the same as without any damping, and the value of p in any mode will be such that

$$\frac{cp + p^2}{1 + \frac{g}{\omega} p} = -\omega_{ko}^2 \quad (9)$$

where ω_{ko} is the undamped natural frequency in the k th mode. Setting $p = -d_k + i\omega_k$, equation (9) implies

$$d_k = \frac{c}{2} + \frac{g}{2} \frac{\omega_{ko}^2}{\omega_k} \quad (10a)$$

where

$$4\omega_k^4 + (c^2 - 4\omega_{ko}^2)\omega_k^2 + 2cg\omega_{ko}^2\omega_k + g^2\omega_{ko}^4 = 0 \quad (10b)$$

To first powers of g ,

$$\omega_k = \omega_{ko} - \frac{cg}{4} \frac{\omega_{ko}^2}{\omega_{ko}^2} \quad (11)$$

where $\omega_{kc} = [\omega_{ko}^2 - (c/2)^2]^{1/2}$ is the natural frequency in the k th mode for $g = 0$. In the case of internal damping only ($c = 0$), equations (10a) and (10b) yield:

$$d_k = \frac{g\omega_{ko}}{\sqrt{2}} \left[1 + (1 - g^2)^{1/2} \right]^{-1/2} = \frac{\omega_{ko}}{\sqrt{2}} [1 - (1 - g^2)^{1/2}]^{1/2} \quad (12a)$$

$$\omega_k = \frac{\omega_{ko}}{\sqrt{2}} [1 + (1 - g^2)^{1/2}]^{1/2} \quad (12b)$$

References

- 1 Lord Rayleigh, "Theory of Sound," vol. 1, Dover Publications, New York, N. Y., pp. 130-131.
- 2 T. K. Caughey, "Classical Normal Modes in Damped Linear Dynamic Systems," *JOURNAL OF APPLIED MECHANICS*, vol. 27, Trans. ASME, vol. 82, Series E, June, 1960, pp. 269-271.
- 3 M. Morduchow, "On Internal Damping of Rotating Beams," NACA Technical Note 1996, December, 1949.
- 4 M. Morduchow, "On Application of a Quasi-Static Variational Principle to a System With Damping," *JOURNAL OF APPLIED MECHANICS*, vol. 21, Trans. ASME, vol. 76, March, 1954, pp. 8-10.

³ In [4] it has been shown that a necessary, as well as sufficient, condition that the mode shapes be entirely unaffected by a damping load of the form $f(x)\partial Y/\partial t$ is that $f(x)$ be proportional to $\rho(x)$.